PolyPublie
Polytechnique Montréal

POLYTECHNIQUE MONTRÉAL
UNIVERSITÉ D'INGÉNIERIE

Titre: Title:	Experimental and Analytical Stress and Strain Characterization of Notched Composite Plates
Auteur: Author:	Aouni Jr. Lakis
Date:	2020
Type:	Mémoire ou thèse / Dissertation or Thesis
Référence: Citation:	Lakis, A. J. (2020). Experimental and Analytical Stress and Strain Characterization of Notched Composite Plates [Master's thesis, Polytechnique Montréal]. PolyPublie. https://publications.polymtl.ca/5577/

Document en libre accès dans PolyPublie
Open Access document in PolyPublie

URL de PolyPublie: PolyPublie URL:	https://publications.polymtl.ca/5577/
Directeurs de recherche: Advisors:	Rachid Boukhili
Programme: Program:	Génie mécanique

Ce fichier a été téléchargé à partir de PolyPublie, le dépôt institutionnel de Polytechnique Montréal
This file has been downloaded from PolyPublie, the institutional repository of Polytechnique Montréal

https://publications.polymtl.ca

POLYTECHNIQUE MONTRÉAL
affiliée à l'Université de Montréal

Experimental and Analytical Stress and Strain Characterization of Notched Composite Plates

AOUNI JR. LAKIS
Département de génie mécanique

Mémoire présenté en vue de l'obtention du diplôme de *Maîtrise ès sciences appliquées*

Génie mécanique

Décembre 2020

© Aouni Jr. Lakis, 2020.

POLYTECHNIQUE MONTRÉAL

affiliée à l'Université de Montréal

Ce mémoire intitulé :

Experimental and Analytical Stress and Strain Characterization of Notched Composite Plates

présenté par **Aouni Jr. LAKIS**

en vue de l'obtention du diplôme de *Maîtrise ès sciences appliquées*

a été dûment accepté par le jury d'examen constitué de :

Aurelian VADEAN, président

Rachid BOUKHILI, membre et directeur de recherche

Louis LABERGE LEBEL, membre

DEDICATION

Dedicated to my parents.

ACKNOWLEDGEMENTS

I would like to express my gratitude to my supervisor, Professor Rachid Boukhili, for his guidance, support and accepting me as one of his students. I would also like to thank him for his great sense of humor during trying times.

A special thanks to Masoud Mehrabian, who has dedicated an enormous amount of his time to help me with my thesis from the beginning until the very end. Manufacturing and testing of the specimens investigated in this research would not have been possible without him.

RÉSUMÉ

Cette recherche a pour but de caractériser la distribution des contraintes, les facteurs d'intensité de contraintes (SCF) et la déformation des trous des échantillons testés selon la norme ASTM D5766 (Open-Hole Tension : OHT) et la norme ASTM D6742 (Filled-Hole Tension : FHT). Les stratifiés composites étaient fabriqués par le procédé d'infusion de résine. Ils étaient composés de tissus carbone taffetas 3K dans une matrice époxy. L'étude englobe l'effet de la séquence d'empilement quasi-isotrope (QI) et croisés (CP) et l'effet de l'épaisseur (8 plis et 12 plis). La distribution des contraintes sur la surface des échantillons de composites est calculée expérimentalement en utilisant les déformations provenant de la corrélation digitale des images (DIC) combinées avec la théorie des stratifiées. Les dimensions caractéristiques des matériaux, l'estimation de la résistance à la traction et les facteurs de contraintes sont calculés en utilisant les critères de Whitney and Nuismer PSC (Point Stress Criterion) et ASC (Average Stress Criterion). Les distributions des contraintes expérimentales sont validées en utilisant le model analytique de Lekhnitskii pour les matériaux anisotropes. En plus, les facteurs des concentrations des contraintes expérimentales pour CP et QI sont comparés avec ceux calculés par le PSC et ASC. La déformation des trous est analysée dans la direction longitudinale et transversale par le DIC en utilisant des extensomètres virtuels.

Les OHT CP qui sont plus minces ont une meilleure capacité de distribution des contraintes que ceux des CP plus épaisses. L'inverse est vrai pour les stratifiées QI. Ceux qui sont plus épaisses ont une meilleure capacité de distribution des contraintes que les plus minces. Quand le trou est fermé par un boulon, la capacité de distribution des contraintes pour CP et QI devient approximativement égale, ce que veut dire que l'introduction d'un boulon annule les effets que le type des stratifiées ont sur la distribution des contraintes.

Le PSC donne une très bonne approximation du SCF pour toutes les stratifiées analysées. Le ASC donne des erreurs de 10% pour le OHT et 18% pour le FHT dans les CP, mais l'estimation de SCF du QI avec le ASC est aussi bonne que le PSC. Le PSC surestimes et le ASC sous-estimes le SCF quand ils sont comparés aux résultats expérimentaux.

La déformation longitudinale du trou (LHE) pour le CP est plus grande que celle du QI et la déformation en compression transversale (THC) est plus petite pour le CP que le QI. Ceci veut dire que le trou de CP s'allonge plus mais il se comprime moins qu'un trou dans une stratifiée QI. Ce

phénomène pourrait être expliqué par le fait que la présence des plis de 45º dans le stratifié quasi-isotrope induit une distribution des déformations maximales dans une forme de papillon. Ceci contribue plus à la compression transversale du trou que son élongation longitudinale. À la connaissance de l'auteur, la caractérisation de la déformation des trous entre les stratifiées de CP et QI n'est pas documentée dans la littérature.

ABSTRACT

The purpose of this work is to characterize the stress distribution, stress concentration factors and the hole deformation of open- and filled-hole (OHT and FHT) cross-ply (CP) and quasi-isotropic (QI) composite plates subjected to uniaxial in-plane loading. Plates of varying thicknesses containing a centrally-located circular through-hole are studied. The stress distribution of notched composite plates is calculated and analyzed experimentally using digital image correlation (DIC) strains combined with laminate theory. For validation, the experimental stress distribution results are compared with those of Lekhnitskii's analytical model for anisotropic materials. The material-dependent characteristic dimensions, predicted strength and stress concentration factors (SCF) are calculated using the point stress criterion (PSC) and the average stress criterion (ASC). In addition, the experimental stress concentration factors for cross-ply and quasi-isotropic laminates are compared to results from analytical solutions based on the PSC and ASC. Notch deformation in both the longitudinal and transversal direction is measured using DIC strains obtained using virtual extensometers.

Thinner OHT CP laminates were found to be better at distributing stress away from the notch than thicker CP laminates; whereas, thicker OHT QI laminates are better at distributing stress than thinner QI laminates. Filling the notch with a tightened bolt was observed to bring the stress distribution capabilities of CP and QI laminates in line with one other; the presence of the bolt nullifies any effect that a layup or laminate thickness may have on stress distribution.

The PSC provides a very good approximation of SCFs for all laminates investigated. Using the ASC to analyze CP laminates induces errors greater than 10% for OHT and 18% for FHT. However, the ASC estimates the SCFs of QI laminates just as well as the PSC. The PSC overestimates and the ASC underestimates the SCF values when compared to experimental results.

The longitudinal hole elongation (LHE) of CP layups is greater than that of QI layups and the transversal hole compression (THC) is less in CP than QI. In other words, a cross-ply notch elongates more and compresses less than a quasi-isotropic notch. This phenomenon may be explained by the fact that the inclusion of 45º plies in a quasi-isotropic layup induces a butterfly distribution of peak strains around the notch area, which contributes more to the transversal compression of the notch than its longitudinal elongation when compared to a cross-ply layup. To

the author's knowledge the difference in notch deformation between CP and QI layups has not yet been documented in the literature.

TABLE OF CONTENTS

DEDICATION III

ACKNOWLEDGEMENTS IV

RÉSUMÉ V

ABSTRACT VII

TABLE OF CONTENTS IX

LIST OF TABLES XI

LIST OF FIGURES XII

LIST OF SYMBOLS AND ABBREVIATIONS XIV

LIST OF APPENDICES XVIII

CHAPTER 1 INTRODUCTION 1

1.1 Overview 1

1.2 Research Objective and Sub-Objectives 2

1.3 Thesis Organization 3

CHAPTER 2 LITERATURE REVIEW 5

2.1 Notched Tensile Strength 5

2.2 Stress Concentration Factors and Stress Distribution 11

2.2.1 Analytical Stress Distribution 11

2.2.2 Analytical Stress Concentration Factors 13

2.2.3 Digital Image Correlation Applied to Notched Composites 18

2.3 Literature Review Key Takeaways 24

CHAPTER 3 METHODOLOGY 26

3.1 Experimental Procedure 26

3.2 Calculating Stress Distribution and Stress Concentration 31

3.3 Notch Deformation Data Retrieval 34
CHAPTER 4 RESULTS AND DISCUSSION 35
4.1 Open- and Filled-Hole Tensile Strength 35
4.2 Stress Distribution from the Notch Edge to the Free Edge 37
4.3 Stress Concentration Factors and Notch Deformation 44
4.3.1 Stress Concentration Factors 44
4.3.2 Notch Deformation 46
CHAPTER 5 CONCLUSION AND RECOMMENDATIONS 51
5.1 Conclusion 51
5.2 Limitations 54
5.3 Recommendations 54
BIBLIOGRAPHY 55
APPENDICES 58

LIST OF TABLES

Table 2.1 : Average failure stress of sub-laminate-level scaled specimens [1] 6

Table 2.2 : Average failure stress of ply-level scaled specimens [1] 6

Table 2.3: Tensile strength of unnotched (TS), OHT, FHT, single lap bolted joints (BJ) and pin-loaded (PLT) for CFRE, GFRE and Al-6065 [5] 10

Table 2.4: Experimental, analytical and numerical SIF results [19] 17

Table 2.5: SCF for plates with different fiber orientation angles under tensile load [22] 21

Table 2.6: Effect of hole eccentricity on stress and strain concentration factors [25] 24

Table 3.1: Laminate configurations and thickness 27

Table 4.1: Stress gradient between 8mm and 16mm from the center of the notch for OHT and FHT specimens at 95% maximum load 43

Table 4.2: Open- and filled-hole strength predictions and characteristic lengths according to the PSC and ASC 45

Table 4.3: Open- and filled-hole experimental stress, PSC and ASC concentration factors 45

Table 4.4: Global longitudinal elongation and local hole elongation of open- and filled-hole laminates at 40% OHT/TS & FHT/TS 48

LIST OF FIGURES

Figure 2-1: Damage progression in CFRP and GFRP quasi-isotropic OHT laminates [2] 7

Figure 2-2: Damage progression in CFRP and GFRP OHT laminates [2] 8

Figure 2-3: Progressive failure of a cross-ply double-edge-notch specimen (% maximum load) [3] 9

Figure 2-4: Progressive failure of a quasi-isotropic double-edge-notch specimen (% maximum load) [3] 9

Figure 2-5: Effect of a tightened bolt on the notch strength [6].....11

Figure 2-6: Stress concentration variation from the notch boundary to the free edge of a composite laminate under uniaxial tension.....12

Figure 2-7: Experimental vs. analytical notch strength in respect to notch diameter [1] 16

Figure 2-8: Image Correlation between a reference and deformed image 19

Figure 2-9: Stress distribution of a woven fabric composite subject to a tensile load [21] 20

Figure 2-10: DIC engineering strain contour plots [22].....21

Figure 2-11: The strain distribution including: (a) circumferential strain, (b) radial strain and (c) shear strain [23] 22

Figure 2-12: Strain variation along sampling path for different hole sizes [23] 22

Figure 2-13: Strain field contours of DIC and FEM at a load of 68.88% of UTS [24] 23

Figure 2-14: Diagram of hole eccentricity with respect to load direction (i.e. x-axis) [25].....24

Figure 3-1: Vacuum-assisted resin infusion setup (before resin infusion).....26

Figure 3-2: Vacuum-assisted resin infusion setup (after resin infusion) 27

Figure 3-3: Open-hole and filled-hole specimen dimensions (all dimensions in mm) 28

Figure 3-4: DIC speckle patterns a) OHT specimen b) FHT specimen 29

Figure 3-5: Uniaxial tensile test setup with DIC cameras.....30

Figure 3-6: Reference points in VIC 3D-7 to obtain strain data 31

Figure 3-7: Application of virtual extensometers in VIC-3D a) OHT b) FHT 34

Figure 4-1: Average tensile strength of unnotched (TS), open-hole (OHT) and filled-hole (FHT) of cross-ply and quasi-isotropic 8- and 12-layer laminates 35

Figure 4-2: Stress-strain and force-strain curves of open- and filled-hole laminates a) OHT stress-strain b) FHT stress-strain 36

Figure 4-3: Analytical vs. experimental normal stress near the notch boundary to the free edge of the specimen at 25% max load for cross-ply 8 & 12 layer and quasi-isotropic 8 & 12 layer OHT specimens 38

Figure 4-4: Strain plots in the axial direction (εxx [%]) at 25% max load for OHT cross-ply and quasi-isotropic 8- & 12- layer laminates 39

Figure 4-5: DIC normalized stress distribution from the notch edge to the free edge of open- and filled-hole specimens a) OHT at 95% max load b) FHT at 95% max load 40

Figure 4-6: Strain contour plots in the axial direction (εxx [%]) at 95% of the maximum load (ML) for cross-ply open- and filled-hole 8 layer laminates (CP8) 41

Figure 4-7: Strain contour plots in the axial direction (εxx [%]) at 95% of the maximum load (ML) for cross-ply open- and filled-hole 12 layer laminates (CP12) 41

Figure 4-8: Strain contour plots in the axial direction (εxx [%]) at 95% of the maximum load (ML) for quasi-isotropic open- and filled-hole 8 layer laminates (QI8).....42

Figure 4-9: Strain contour plots in the axial direction (εxx [%]) at 95% of the maximum load (ML) for quasi-isotropic open- and filled-hole 12 layer laminates (QI12).....42

Figure 4-10: The effect of laminate layup on open- and filled-hole notch deformation a) OHT - longitudinal hole elongation b) OHT - transversal hole compression c) FHT - longitudinal hole elongation d) FHT - transversal hole compression 47

Figure 4-11: Normalized stress vs. global longitudinal elongation a) OHT - global longitudinal elongation b) FHT - global longitudinal elongation.....47

Figure 4-12: Longitudinal and transversal strain contours at 40% OHT/TS for CP12 and QI12..50

Figure B-1: Equivalent Laminate Theory 64

LIST OF SYMBOLS AND ABBREVIATIONS

2D	Two dimensional
3D	Three dimensional
ASC	Average stress criteria
CP8	Cross-ply 8-layer laminate
CP12	Cross-ply 12-layer laminate
DIC	Digital image correlation
FHT	Filled-hole tension
FWC	Finite width correction
GLE	Global longitudinal elongation
LHE	Longitudinal hole elongation
ML	Maximum load
OHT	Open-hole tension
PSC	Point stress criteria
QI8	Quasi-isotropic 8-layer laminate
QI12	Quasi-isotropic 12-layer laminate
SCF	Stress concentration factor
THC	Transversal hole compression
TS	Unnotched tension specimen
VARI	Vacuum assisted resin infusion
VE	Virtual extensometer
$A_{11} \dots A_{66}$	Constituents of the extension stiffness matrix
[A]	Extension stiffness matrix

a_0	The characteristic length for the average stress criteria
$B_{11} \dots B_{66}$	Constituents of the coupling stiffness matrix
$[B]$	Coupling stiffness matrix
d_0	The characteristic length for the point stress criteria
D	Hole diameter
$[D]$	Bending stiffness matrix
$\Delta\sigma$	Stress gradient between the stress at the notch and free edge of the laminate
$\Delta\sigma_{50\%}$	Stress gradient at 50% of the maximum load
$\Delta\sigma_{95\%}$	Stress gradient at 95% of the maximum load
E_{11}	Lamina longitudinal Young modulus
E_{22}	Lamina transversal Young modulus
E_f	Fiber Young modulus
E_m	Matrix Young modulus
$\overset{\circ}{\varepsilon_{xx}}$	Experimental strain in the normal (axial) direction
$\overset{\circ}{\varepsilon_{yy}}$	Experimental strain in the transversal direction
G	Shear modulus for an isotropic material
G_{12}	Lamina in-plane shear modulus
G_f	Fiber shear modulus
G_m	Matrix shear modulus
h	Plate thickness
h_j	Distance from the midplane of the laminate to the top of the j^{th} lamina
h_{j-1}	Distance from the midplane of the laminate to the bottom of the j^{th} lamina
$K_{\frac{\pi}{2}}$	Stress concentration factor

K_T^{∞}	Stress concentration factor for an infinite width plate
K_T	Stress concentration factor for a finite width plate
$K_{\frac{\pi}{2}}^{PSC}$	Stress concentration factor from the point stress criteria
$K_{\frac{\pi}{2}}^{ASC}$	Stress concentration factor from the average stress criteria
$K_{\frac{\pi}{2}}^{EXP}$	Experimental stress concentration factor
N	Total number of laminas in a laminate
N_{xx}	Force per unit length in the normal (axial) direction
V_f	Fiber volume fraction
V_m	Matrix volume fraction
υ_f	Fiber Poisson ratio
υ_m	Matrix Poisson ratio
υ_{12}	Lamina longitudinal Poisson ratio
υ_{21}	Lamina transversal Poisson ratio
ξ_1	The ratio of radius to characteristic length of the point stress criteria
ξ_2	The ratio of radius to characteristic length of the average stress criteria
$Q_{11} \dots Q_{66}$	Constituents of the stiffness matrix for a specially orthotropic lamina
$\bar{Q}_{11} \dots \bar{Q}_{66}$	Constituents of the stiffness matrix for a general orthotropic lamina
$[Q]$	Stiffness matrix for a specially orthotropic lamina
$[\bar{Q}]$	Stiffness matrix for a general orthotropic lamina
r	Hole radius
$U_1 \dots U_6$	Angler-invariant stiffness properties
w	Plate width
$\sigma_x(0, y)$	Normal stress from the notch edge to the free edge of the laminate along the y-axis

σ^{∞}	Uniform applied stress
σ_N^{∞}	Normal stress for an infinite width plate
σ_N	Normal stress for a finite width plate
σ_f	Tensile strength of the unnotched laminate for the point and average stress criteria
σ_{OHT}	Tensile strength of open-hole tension laminates
σ_{FHT}	Tensile strength of filled-hole tension laminates
σ_{TS}	Tensile strength of unnotched laminates
σ_{xx}	Experimental normal stress
σ_{Free}	Normal stress at the free edge of the laminate
σ_{Notch}	Normal stress at the boundary of the notch edge
Y	Finite width correction factor

LIST OF APPENDICES

Appendix A: Additional Strain Contour Plots 58

Appendix B: Material Properties.....59

CHAPTER 1 INTRODUCTION

1.1 Overview

Advanced composite materials are widely used in a variety of industries, especially in the aerospace domain. This can be attributed to their compelling advantages over isotropic materials, such as high strength and stiffness-to-weight ratios, low density, low thermal expansion and designable characteristics for lightweight efficient structures. During the past few decades, these characteristics have led to a rapid increase in use of these materials for structural applications. Structural elements made of advanced fiber-reinforced composite materials are now used extensively in high and low technology areas, including the aerospace industry, where complex shell-type configurations are common structural elements. In general, these materials are fiber-reinforced laminate, symmetric or antisymmetric cross- and angle-ply, composed of numerous layers with varied fiber orientations. Although the total laminate may exhibit orthotropic-like properties, each layer of the laminate is usually anisotropic, and therefore the individual properties of each layer must be considered when attempting to gain insight into the actual stress and strain fields. By optimizing the properties during the design phase, the overall weight of a structure can be reduced since stiffness and strength can be incorporated only where they are required. A lower weight structure translates into higher performance. Since optimized structural systems are often more sensitive to instabilities, it is necessary to exercise caution. The designer would be much better able to avoid any instabilities if, when predicting a maximum load capacity, the equilibrium paths of structural elements were known or accurate modelling of the load-displacement behavior and stress distribution of the structure was available.

Composites have great design flexibility because they may be molded into very complex shapes. This effectively reduces the number of joints in a given structure, which results in a lighter weight and fewer stress concentration regions. Some joints are still necessary however, and mechanically fastened joints are commonly used. The presence of a joint creates discontinuity in a member, which affects stress distribution and acts as a region of stress concentration. Holes are necessary for fastened joints and it is therefore imperative to understand the effect of their presence on the mechanical integrity of composite plates.

Use of composite plates often requires that cutouts, especially circular or elliptical holes, be drilled into the laminate to facilitate joining structural parts or provide access to the interior of thin-walled structures such as aircraft wings. Cutouts are typically used for passage of electronic wires, hydraulic pipes, or to facilitate the assembly operations. These holes could cause stress concentrations in the vicinity of structural discontinuities, resulting in a significant reduction of load-carrying capacity, strength, and service life of the composite structures. The integrity and continuity of fiber and matrix in the composite plate are destroyed when a hole is drilled, and consequently the notch region is not only the weakest part of the structure, but serious stress concentrations occur in the area. Accurate analysis of local stress level and damage evolution of notched laminated shell-type structures are of great importance to allow composite materials to be used for engineering applications. The behavior of laminated composite plates with stress concentration around the open holes has therefore received special attention by researchers and engineering designers.

It is recognized that plane wave fabrics [0/90] are commonly used in the composites industry due to their ease of manufacturing and advantageous performance-to-cost ratio. Studying the cross-ply configuration can be justified for comparison purposes with other studies. However, if rigidity along the 45-degree axis is required or if the structure will experience torsional stress, then a quasi-isotropic configuration provides superior performance. This requires turning [0/90] woven plies 45 degrees. It will be shown that there are few studies that have been made on the characterization of stress distribution capabilities and notch deformation between OHT and FHT specimens of cross-ply and quasi-isotropic layups. Although stress concentration factors are of great importance and have been studied extensively, they are not necessarily representative of the capability of a laminate to redistribute the stress away from the notch. As well, stress concentration factors do not shed light on how a notch may deform in both longitudinal and transversal directions.

1.2 Research Objective and Sub-Objectives

The objective of this thesis is to characterize the stress distribution and notch deformation for the case of open-hole (OHT) and filled-hole (FHT) cross-ply and quasi-isotropic carbon-fiber reinforced epoxy composite plates. There has been extensive research done in the domain of analyzing stress concentration between the two lay-ups, as well as characterizing damage progression (as will be described in Chapter 2: Literature Review). However, to the author's

knowledge there has not been an attempt to describe and investigate the difference in stress distribution capabilities between the two lay-ups with and without a clamped bolt. Furthermore, it seems that an analysis of the difference in notch deformation between cross-ply and quasi-isotropic laminates has not been presented in the literature. This work will be conducted with the following sub-objectives (SO):

- SO1: Characterize the notch strength of both OHT and FHT specimens
- SO2: Characterize the stress distribution capabilities of each specimen
- SO3: Characterize the stress concentration factors of each specimen
- SO4: Characterize the notch deformation in both longitudinal and transversal directions of each specimen

1.3 Thesis Organization

This thesis is divided into 5 Chapters. The content in each chapter is described as follows:

- CHAPTER 2: Literature Review
    - A summary of past research on the study of notched composite plates including the study of notched tensile strength, damage progression, analytical models for the prediction of strength and stress concentration factors and utilization of the DIC technique for analysis of strain and stress concentrations.
- CHAPTER 3: Methodology
    - An in-depth explanation of the following:
        - 1) Manufacturing of both the OHT and FHT specimens (sub-objective 1)
        - 2) Testing of the OHT and FHT specimens (sub-objective 1)
        - 3) Procedure for calculating the experimental stress concentration factors as well as the stress distribution from the notch edge to the free edge of each specimen using DIC strains (sub-objectives 2 and 3)
        - 4) Procedure for obtaining experimental notch deformation in both longitudinal and transversal directions (sub-objective 4)

- CHAPTER 4: Results and Discussion
    - Analysis and discussion of the stress distribution, stress concentration factors and notch deformation results of the specimens investigated
- CHAPTER 5: Conclusion, Limitations and Recommendations
    - Summary of work completed as well as the sub-objectives that have been met
    - Limiting factors attributed to the research
    - Potential future work

CHAPTER 2 LITERATURE REVIEW

Geometrical discontinuities, such as notches, grooves, or holes, are unavoidably present in engineering structural systems, and are often responsible for crack formation and propagation under static and cyclic loading.

It is known that the stress concentration around an open circular hole in an infinite isotropic plate subject to uniform in-plane tensile load is three times that of the applied stress and this value could be higher with an elliptical hole. The stress concentrations for composite structures can be much more severe due to material anisotropy. At the same time, the low ductility of composites makes them very sensitive to stress concentration and failures can easily occur when high stress reaches the proportional limit.

Drilled holes introduce the further stress concentrations which significantly reduce the fracture strength of structural components loaded in either tension or compression.

2.1 Notched Tensile Strength

The notch tensile strength is the ultimate stress that a notched composite specimen under uniaxial tension reaches before failure. Studying the notch tensile strength is important for the following two reasons:

1) The failure mechanism and damage progression that occur as stress is applied to laminates tend to be exaggerated due to the stress concentration region.
2) Studying the OHT strength of composite laminates is the most straightforward and easiest approach to understanding the region of stress concentration in bolted joints.

Green et al. [1] studied the tensile strength of notched non-woven quasi-isotropic composite plates. They illustrated the effect that laminate thickness and hole size has on the notch strength. Ply-level and sub-laminate-level scaling methods were used for thickening of the laminates. Ply-level scaling involves increasing the number of plies of the same orientation blocked together, whereas sub-laminate-level scaling is the act of increasing the number of sub-laminates. Table 2.1 illustrates that as the laminate thickness (t) increases by sub-laminate-level scaling, the notched tensile strength decreases for a given hole diameter. The same effect can be seen for ply-level scaling in Table 2.2 but at a more pronounced rate as the tensile strength decreases by 64% when the laminate

thickness increases from 1mm to 8mm for a notch radius of 3.175mm. Comparatively, the tensile strength decreases by only 16% using sub-laminate level scaling for the same increase in thickness. Therefore, as laminate thickness increases the notched tensile strength decreases and ply-level scaling has a more severe effect on the tensile strength than that of sub-laminate-level scaling.

Table 2.1 : Average failure stress of sub-laminate-level scaled specimens [1]

Average failure stress of sublaminate-level scaled specimens (MPa) (cv, %)				
t (mm)	Hole diameter (mm)			
	3.175	6.35	12.7	25.4
1	570 (7.69)			
2	500 (3.95)	438 (2.44)		
4	478 (3.09)	433 (2.03)	374 (1.01)	331 (2.98)
8	476 (5.06)			332 (1.31)

Table 2.2 : Average failure stress of ply-level scaled specimens [1]

Average failure stress of ply-level scaled specimens (MPa) (cv, %)				
t (mm)	Hole diameter (mm)			
	3.175	6.35	12.7	25.4
1	570 (7.69)			
2	396 (5.18)	498 (6.45)		
4	275 (5.56)	285 (5.17)	362 (2.60)	417 (4.10)
8	202 (7.90)			232 (1.87)

The decrease of notched tensile strength with an increase in laminate thickness is due to the increase of 0^{o} plies within the laminate; which aid in reducing the propagation of damage through the thickness. This damage is also known as sub-critical damage and may take the form of axial-splitting, matrix cracking and/or delamination. The decrease in damage results in less stress relief and therefore the tensile strength is reduced.

O'Higgins et al. [2] investigated the open-hole tension (OHT) characteristics of glass and carbon fiber-reinforced composite materials and showed similar results to those presented in [1]. However,

a more in-depth analysis into the damage progression was analyzed [2] for OHT specimens, including cross-ply (CP) and quasi-isotropic (QI) layups by taking x-ray photos at different load levels to failure. Quasi-isotropic laminates were seen to exhibit matrix cracking within $\pm 45^{o}$ and 90^{o} plies at the notch boundary. This damage was then followed by triangular delamination at the hole vicinity which leads to plie decoupling. This damage phenomenon can be seen in Figure 2-1 for carbon-fiber reinforced plastic (CFRP) and glass-fiber reinforced plastic (GFRP).

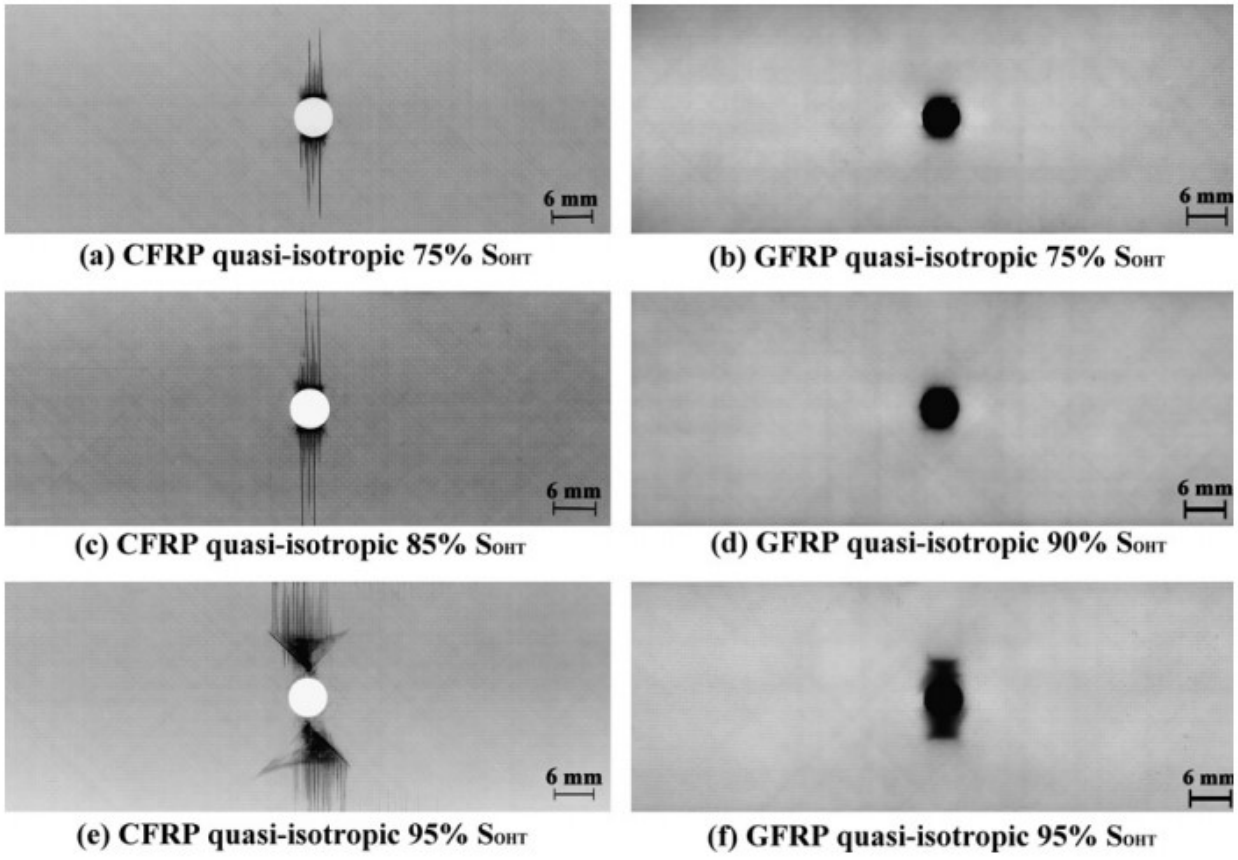

Figure 2-1: Damage progression in CFRP and GFRP quasi-isotropic OHT laminates [2]

The damage progression in cross-ply laminates was different and is illustrated in Figure 2-2. Axial splits occur at the hole boundary due to the 0^{o} plies within cross-ply layups. This damage is then followed by matrix cracking in the 90^{o} plies. Both cross-ply and quasi-isotropic laminates exhibit matrix cracking in the 90^{o} plies, however axial splitting is only seen within cross-ply layups. It is important to note that matrix cracking in cross-ply laminates only occurs outside the axial splitting

located at the notch boundary. It can therefore be concluded that the axial split within the 0º plies isolates the notch boundary from the matrix cracking accrued in the 90º plies.

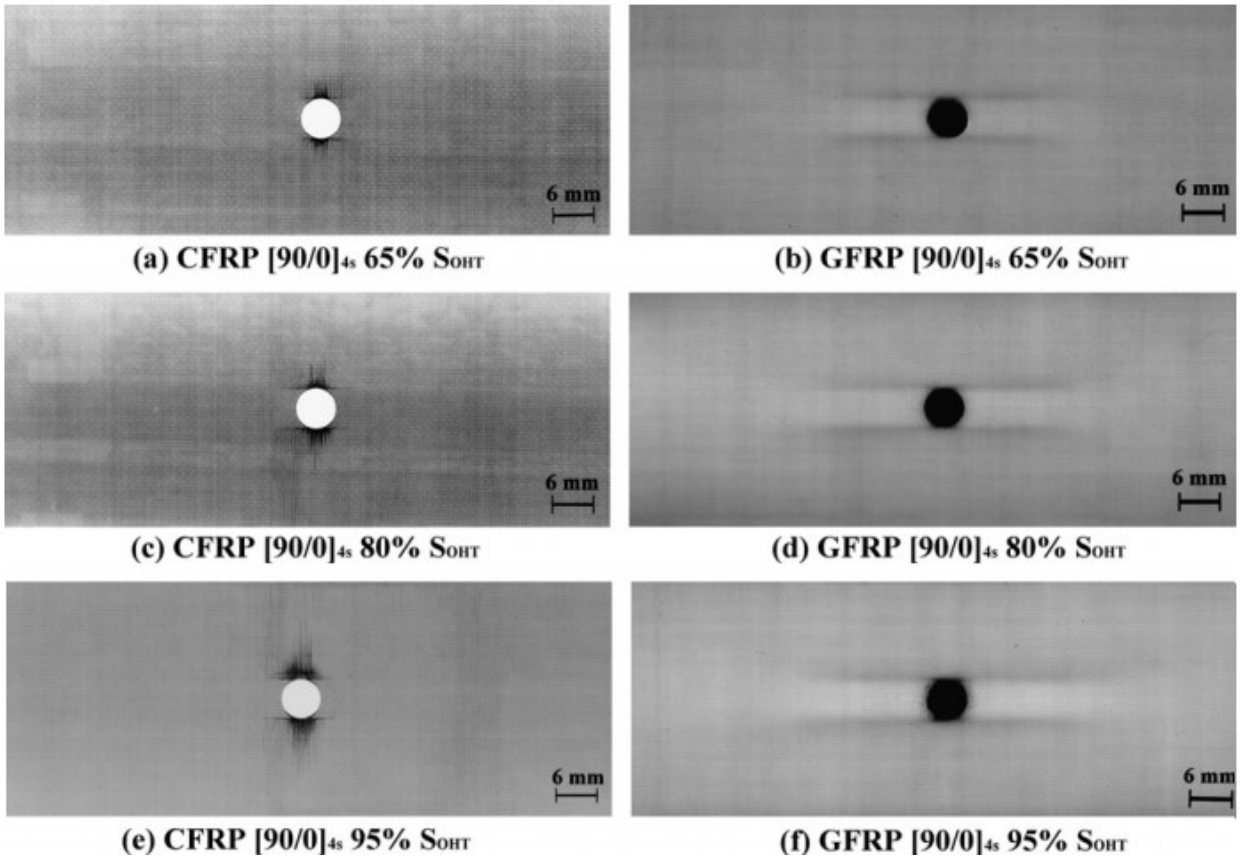

Figure 2-2: Damage progression in CFRP and GFRP OHT laminates [2]

Hallet and Wisnom [3] investigated the effect of laminate layup on the damage progression. Their estimates of notched tensile strength show good agreement with those of [2]. Hallet and Widsom [3] used double-edge-notched specimens instead of OHT specimens, however the progressive damage is like that seen in OHT specimens. The damage progression for CP and QI double-edge-notch specimens can be seen in Figures 2-3 and 2-4, respectively. CP layups exhibit axial splits at the notch edge followed by matrix cracking in the 90º plies and QI layups display matrix cracking in the $\pm$45º and 90º plies. There is a clear distinction between splits and cracks. Splits are initiated at the notch edge and are followed by delamination adjacent to the axial splits. Cracks are distributed evenly throughout the high-stress regions and are usually not accompanied by delamination for double-edge-notched specimens.

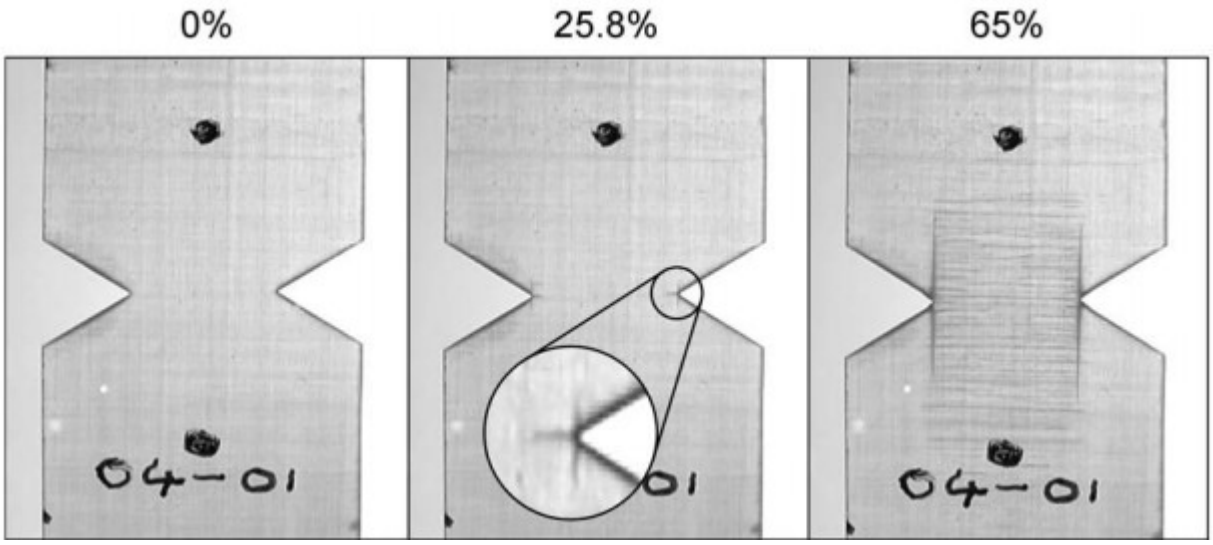

Figure 2-3: Progressive failure of a cross-ply double-edge-notch specimen (% maximum load) [3]

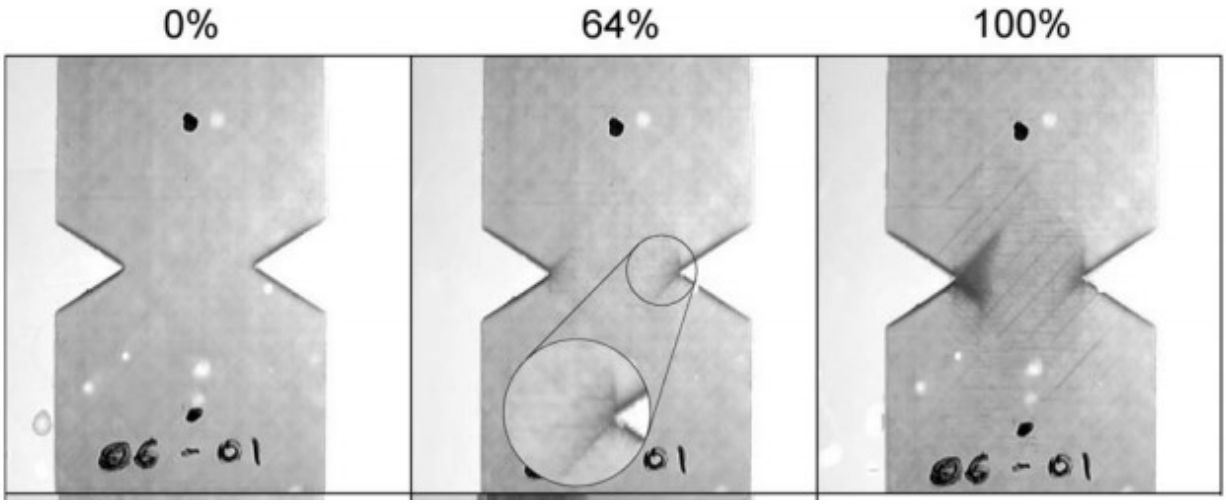

Figure 2-4: Progressive failure of a quasi-isotropic double-edge-notch specimen (% maximum load) [3]

The following key takeaways can be made from the three studies previously mentioned [1-3]:

- As laminate thickness increases, notch strength decreases
- Increasing the number of 0^{o} plies reduces damage progression through the thickness
- Quasi-isotropic laminates exhibit $\pm 45°$ and $90°$ matrix cracking followed by extensive triangular delamination

- Cross-ply laminates exhibit 0° axial splits followed by 90° matrix cracking. The 0° axial splits blunt the stress concentration at the notch boundary.

Understanding the effects of a clamped bolt on the tensile strength of notched composites is equally important, since mechanically-fastened joints are impossible to design without the addition of bolts. Hao et al. [4] studied the effects of open and pin-filled holes on the tensile properties of nonwoven composites and demonstrated that filling the notch with a pin slightly reduces the tensile strength and significantly increases the displacement-to-failure of the specimen.

It cannot be concluded that filling the notch with a pin or a clamped bolt results in a reduction of notch strength. Gamdani et al. [5] found that the OHT strength is usually higher than the filled-hole tension (FHT) strength, although the inverse may occur depending on the conditions. As previously mentioned, damage plays a significant role in the notched strength of a laminate; since the decrease in damage results in less stress relief resulting in a reduction of the tensile strength. Filling the notch with a clamped bolt reduces the amount of damage generated around the notch boundary; therefore, reducing the strength. The condition where FHT strength may be higher than OHT strength can be seen in laminates which are not prone to damage; a bolt-filled hole does not play a role in reducing damage which is not present in the first place. The results from Gamdani's [5] investigation of carbon and glass composites showed that FHT strength was only 3% higher than OHT strength in quasi-isotropic laminates and 7% higher in cross-ply laminates, as shown in Table 2.3.

Table 2.3: Tensile strength of unnotched (TS), OHT, FHT, single lap bolted joints (BJ) and pin-loaded (PLT) for CFRE, GFRE and Al-6065 [5]

Tensile strength of unnotched (TS), OHT, FHT, single lap bolted joints (BJ) and pin-loaded (PLT) for CFRE, GFRE and Al-6065.

		Carbon/epoxy		Glass/epoxy		Al-6065
		Cross-ply	Quasi-isotropic	Cross-ply	Quasi-isotropic	
TS	MPa	500	458	425	359	314
STD		13	26	20	11	5
OHT	MPa	311	316	226	189	267
STD		*6.5*	*8.8*	*3.2*	*3.0*	*1.1*
OHT/TS	ratio	62%	69%	53%	53%	85%
FHT	MPa	331	327	241	232	275
STD		*13.2*	*15.4*	*11.3*	*6.0*	*1.4*
FHT/TS	ratio	66%	71%	57%	65%	88%

Yan et al. [6] investigated the effects of a clamped bolt on notch strength and demonstrated that the effect is negligible for laminates not prone to damage, more specifically delamination. On the other hand, a clamped bolt has a significant effect on the strength of laminates that are prone to delamination as shown in Figure 2-5. One of the main differences found between laminates prone to delamination and those that are not, was that the former had a higher percentage of 0º plies.

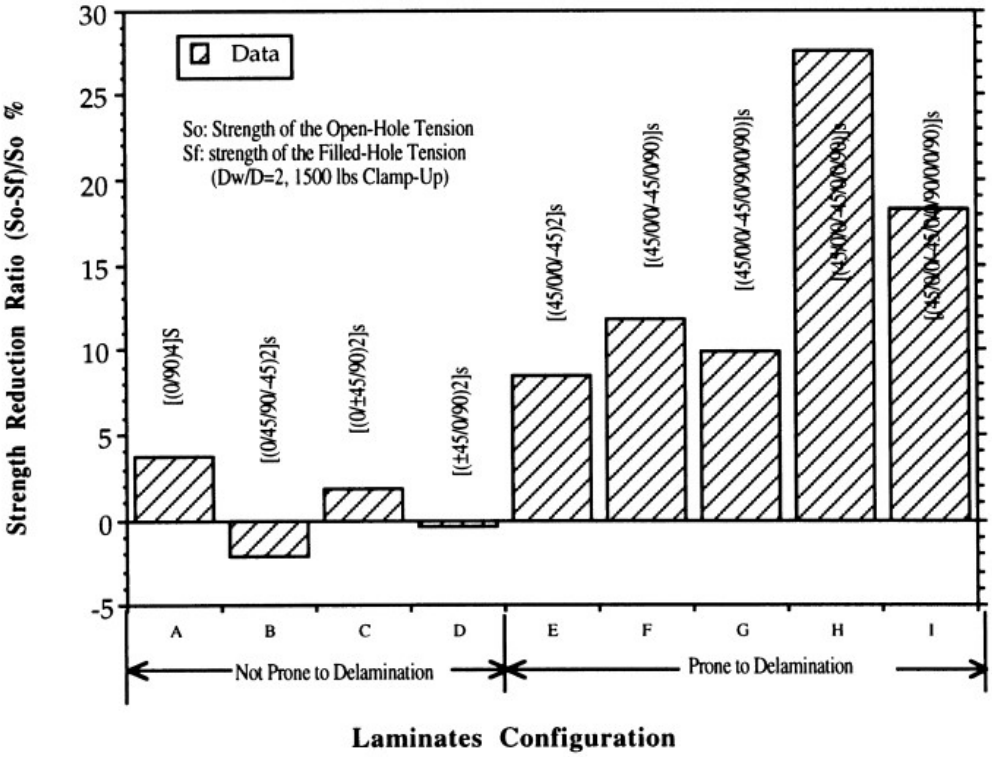

Figure 2-5: Effect of a tightened bolt on the notch strength [6]

2.2 Stress Concentration Factors and Stress Distribution

2.2.1 Analytical Stress Distribution

The stress distribution between the notch boundary and the free edge of a notched composite plate may be estimated by applying Lekhnitskii's analytical model for stress distribution [7].

Consider an infinite anisotropic plate with a circular hole of radius r as shown in Figure 2-6. When the plate undergoes a uniform stress σ^{∞}, the normal stress σ_x oriented in the direction of the x-axis

and on a point along the y-axis perpendicular to the hole boundary can be calculated using the following equation [7]:

If $y \geq r$:

$$\sigma_x(y,0) = \frac{\sigma^\infty}{2}\left\{2 + \left(\frac{r}{y}\right)^2 + 3\left(\frac{r}{y}\right)^4 - (K_T^\infty - 3)\left[5\left(\frac{r}{y}\right)^6 - 7\left(\frac{r}{y}\right)^8\right]\right\} \quad (2.1)$$

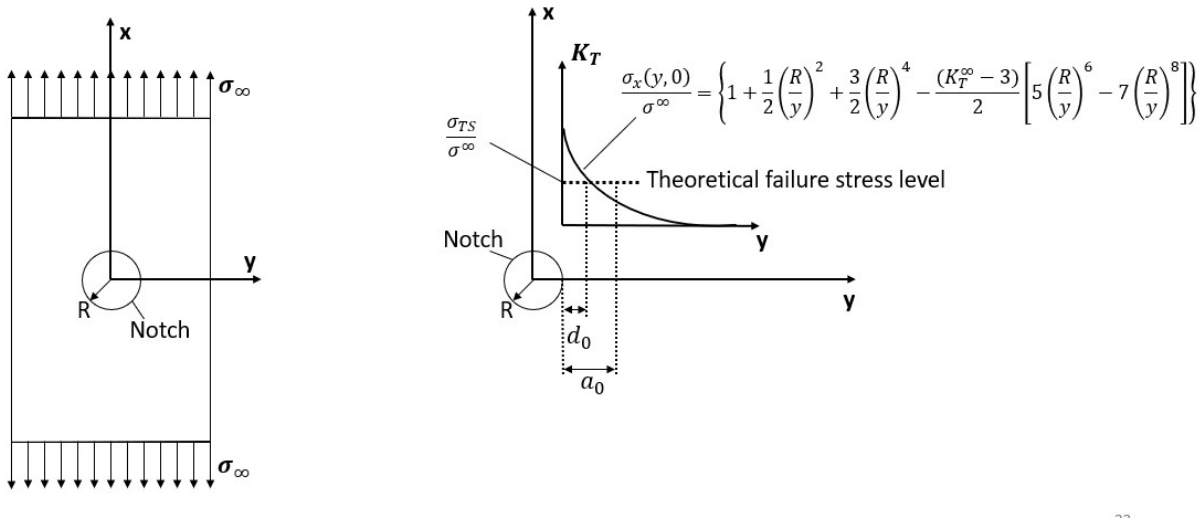

Figure 2-6: Stress concentration variation from the notch boundary to the free edge of a composite laminate under uniaxial tension

The x-axis is the direction of the applied load (the axial direction) and the y-axis is the transversal direction (perpendicular to the x-axis) with the coordinates (0,0) at the center of the notch, as shown in Figure 2-6. Equation (2.1) is dependent on the notch radius (r), the distance from the notch boundary (y) and the stress concentration factor (K_T^∞).

If $y = r$ (at the edge of the hole boundary) then the stress concentration factor is obtained as:

$$K_{\frac{\pi}{2}} = \frac{\sigma_x(r,0)}{\sigma^\infty} = K_T^\infty \quad (2.2)$$

For a symmetric laminate with orthotropic in-plane stiffness properties, K_T^∞ is given by:

$$K_T^{\infty} = 1 + \sqrt{\frac{2}{A_{11}}\left(\sqrt{A_{11}A_{22}} - A_{12} + \frac{A_{11}A_{22} - A_{12}^2}{2(A_{66})}\right)} \tag{2.3}$$

Where terms $A_{11} \cdots A_{66}$ are the constituents of the extension stiffness matrix $[A]$.

2.2.2 Analytical Stress Concentration Factors

A simple analytical model is presented by Whitney and Nuismer [8][9] to predict the stress concentration factors of notched composite plates. The point stress criterion (PSC) and average stress criterion (ASC) are derived from Lekhnitskii's model for stress distribution [7]. The PSC and ASC are useful for predicting the uniaxial tensile strength of laminated composite plates that contain through-the-thickness discontinuities of a general shape. Each criterion is a two-parameter model dependent on the unnotched strength and characteristic length. These can be used to predict the size effects of the observed discontinuity. The characteristic length is assumed to be a material property and therefore is independent of hole size and plate geometry.

Point Stress Criterion (PSC)

The PSC assumes that failure will occur when $\sigma_x(y, 0)$ at a certain distance d_0 from the hole boundary reaches the tensile strength σ_{TS} of the material (which is the tensile strength of the plate without a notch) as seen in Figure 2-6. The PSC is expressed as follows [8][9]:

$$\sigma_x(y = r + d_0, 0) = \sigma_{TS}$$

The stress concentration factor is written as:

$$K_{\frac{\pi}{2}}^{PSC} = \frac{\sigma_x(r + d_0)}{\sigma^{\infty}} = \frac{1}{2}\{2 + \zeta_1^2 + 3\zeta_1^4 - (K_T^{\infty} - 3)[5\zeta_1^6 - 7\zeta_1^8]\} \tag{2.4}$$

Where:

$$\xi_1 = \frac{r}{r + d_0} \tag{2.5}$$

The distance d_0 is considered a material property and is independent of the geometry and hole size (Figure 2-6). The material-dependent parameter d_0 can be obtained using a simple open-hole tension test.

The ratio of notched (σ_{OHT}) to unnotched (σ_{TS}) tensile strength is:

$$\frac{\sigma_{OHT}}{\sigma_{TS}} = \frac{2}{2 + \zeta_1^2 + 3\zeta_1^4 - (K_T^\infty - 3)[5\zeta_1^6 - 7\zeta_1^8]} \tag{2.6}$$

σ_{OHT}, σ_{TS}, K_T^∞ and r are known, and therefore the value of ξ_1 can be calculated using Equation (2.6) and then d_0 can be found using Equation (2.5).

Average Stress Criterion (ASC)

The average stress criterion assumes that failure will occur when the average of $\sigma_y(x, 0)$ over a distance a_0 from the hole boundary reaches the maximum tensile strength σ_{TS} of the material. The ASC is expressed as follows [8][9]:

$$\frac{1}{a_0}\int_r^{r+a_0} \sigma_x(y, 0)dy = \sigma_{TS}$$

The stress concentration factor can be written as:

$$K_{\frac{\pi}{2}}^{ASC} = \frac{\sigma_x(y)}{\sigma^\infty} = \frac{1}{2(1 - \xi_2)}\{2 - \zeta_2^2 - \zeta_2^4 - (K_T^\infty - 3)[\zeta_2^6 - \zeta_2^8]\} \tag{2.7}$$

Where:

$$\xi_2 = \frac{r}{r + a_0} \tag{2.8}$$

The distance a_0 is considered a material property and is independent of geometry and hole size (Figure 2-6). The material-dependent parameter a_0 can be obtained using a simple open-hole tension test.

The ratio of notched (σ_{OHT}) to unnotched (σ_{TS}) tensile strength is:

$$\frac{\sigma_{OHT}}{\sigma_{TS}} = \frac{2(1 - \xi_2)}{2 - \zeta_2^2 - \zeta_2^4 + (K_T^{\infty} - 3)[\zeta_2^6 - \zeta_2^8]} \tag{2.9}$$

σ_{OHT}, σ_{TS}, K_T^{∞} and r are known, and therefore the value of ξ_2 can be calculated from Equation (2.9) and a_0 can then be found using Equation (2.8).

Many researchers have used these criteria as a basis to make progressive modifications to the classical method throughout the years. For example, Pipes et al. [10] extended the two-parameter model proposed by Whitney-Nuismer [9] into a three-parameter notch strength model in which the characteristic length is assumed to be a function of the hole size (as a function of half of the crack length), reference radius, and the notch sensitivity factor. However, no physical basis was found for the characteristic length because the notch sensitivity factor varies depending on selection of the reference radius.

The notched strength and fracture criterion in fabric composite plates containing a circular hole was studied by Kim et al. [11]. They experimentally investigated the effect of hole size and specimen width on the fracture behavior of several woven fabric composite plates under tensile load. According to their results, the characteristic length in the PSC not only depends on the hole size, but also on the specimen width. It was also shown that the characteristic length decreases with an increase in the notched strength.

Awerbuch et al. [12] summarized various fracture models that have been developed for predicting the notched strength of composite laminates. These fracture models are generally categorized into

three groups; a) stress fracture models, b) fracture mechanic models, and c) progressive damage models [13-16]. Among these techniques, stress fracture models are the most widely used due to their simplicity.

Srivastava [17] presented a modified point stress criterion for predicting the notched strength of glass fiber and carbon fiber laminated composites that contain a centrally-located circular or elliptical through-hole, or a center crack. The effects of the size and specimen width on the fracture behavior of several woven composite plates were also investigated.

Accuracy of the PSC and ASC

The application of the ASC by Green [1] demonstrated good agreement when compared to experimental results for sub-laminate level scaling, as seen in Figure 2-7. However, the ASC induces an error greater than 10% for a notch diameter less than 5mm. Using the ASC to predict notch strength for ply-level scaling is not recommended because the analytical results diverge greatly from the experimental results. Green [1] attributes these errors to the fact that the ASC does not account for laminates that exhibit extensive delamination prior to failure (seen within ply-level scaling laminates), which affects the strength.

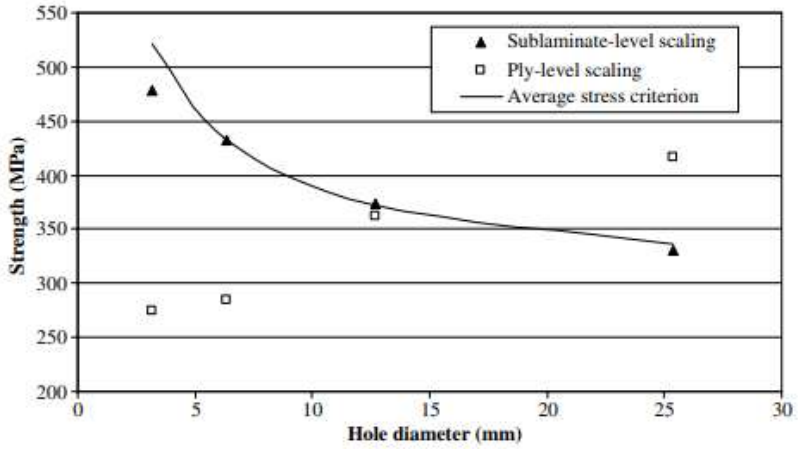

Figure 2-7: Experimental vs. analytical notch strength in respect to notch diameter [1]

Ko's [18] research into stress concentration around small circular holes in composites revealed that anisotropic stress concentration factors (SCFs) could be greater or less than those of isotropic

materials. The point stress and average stress criteria were used, and analytical results compared well with those obtained experimentally. The direction of the tangential stress points changes depending on the fiber orientation with respect to the loading axis.

Dirikolu and Aktas [19] investigated the stress intensity factors (SIFs) of notched composite plates under uniaxial tension utilizing the PSC and a numerical model created in FRANC2D. The accuracy was promising, since the highest margin of error between the two methods was only 6% for a plate with a notch radius of 4mm, as illustrated in Table 2.4.

Table 2.4: Experimental, analytical and numerical SIF results [19]

Experimental, analytical and numerical results

r (mm)	σ_c (MPa)	a_c (mm)	$f(a/r)$	SIF, K_I (MPa$\sqrt{m}$)		
				Waddoups' approach	Point stress criterion	Numerical FRANC2D/L
2	191	0.62	2.15	–	18.08	17.80
3	168	0.55	2.48	18.04	17.22	17.37
4	152	0.55	2.61	–	16.49	17.48
Averages				18.04	17.26	17.55

Finite Width Correction Factor (FWC)

The theory expressed in Lekhnitskii's model [7], as well as the point and average stress criteria is based on an infinite plate width. For a finite-width plate, a finite width correction factor (FWC) must be applied to correct the analytical stress. Tan SC. [20] has come up with the following denotation for the FWC:

$$\frac{K_T}{K_T^{\infty}}\sigma_N^{\infty} = \sigma_N \tag{2.10}$$

Where:

- K_T is the stress concentration for a finite-width plate
- K_T^{∞} is the stress concentration for an infinite-width plate (Equation (2.3))

- σ_N^{∞} is the normal stress for an infinite-width plate (Equation (2.1))
- σ_N is the normal stress for a finite-width plate

The FWC for a circular notched composite plate can be expressed as [20]:

$$Y = \frac{K_T}{K_T^{\infty}} = \frac{\left[2 - \left(\frac{D}{w}\right)^2 - \left(\frac{D}{w}\right)^4\right]}{2} + \frac{\left[\left(\frac{D}{w}\right)^6 (K_T^{\infty} - 3)\left(1 - \left(\frac{D}{w}\right)^4\right)\right]}{2} \tag{2.11}$$

Where:

- D is the hole diameter
- w is the plate width

2.2.3 Digital Image Correlation Applied to Notched Composites

There are a number of ways to experimentally measure the deformation and displacement of materials. Two common tools are extensometers and strain gauges, which provide a local measurement of strain. The digital image correlation (DIC) method provides extensive full-field strain data, which is useful to obtain a more comprehensible understanding of the global and local deformation of a specimen. DIC is especially useful for analyzing deformations that arise from cracking and stress concentrations because it is one of the few techniques able to retrieve strain values near discontinuities (this is beyond the capabilities of extensometers and strain gauges).

The digital image correlation technique is a non-contact optical method; two images are taken before and after loading or at specific time increments. A correlation is found between each image as seen in Figure 2-8. The DIC method can be used either for two-dimensional (2D) or three-dimensional (3D) displacements, which means that the method can capture not only in-plane displacements in the X and Y directions but also out-of-plane displacements in the Z direction.

Figure 2-8 illustrates an example of the correlation between the reference image of subset j and subset center $P(x, y)$ and the deformed image which has now become subset $j'$with subset center

$P'(x', y')$. Tracking of the subset j is performed using cross-correlation or normalized cross-correlation functions. The displacement of the subset center $P(x, y)$ to $P'(x', y')$ is a vector and is illustrated as a blue dashed line in Figure 2-9. Assuming a 2D DIC method is used, the vector can be decomposed into a horizontal displacement (u) and a vertical displacement (v) of the subset, which allows calculation of the resulting strains in the x and y directions.

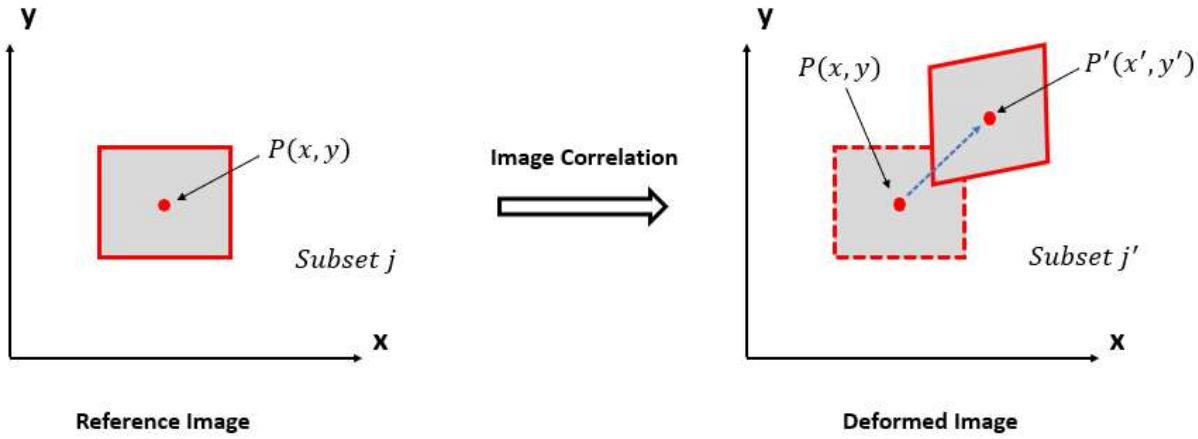

Figure 2-8: Image Correlation between a reference and deformed image

Estimation of stress concentration factors and stress distribution using the electronic speckle pattern interferometer method, a non-contact measurement method of obtaining full-field strain values, was investigated by Toubal et al. [21] for notched composite plates. Their experimental results were compared to those calculated using a finite element model and Lekhnitskii's analytical model [7] for anisotropic materials. A comparison of stress distribution from the notch boundary to the free edge of the specimen for each of the three methods is shown in Figure 2-9. The research concluded that using a non-contact method to calculate stress distribution is appropriate since the results compared well with analytical and numerical models.

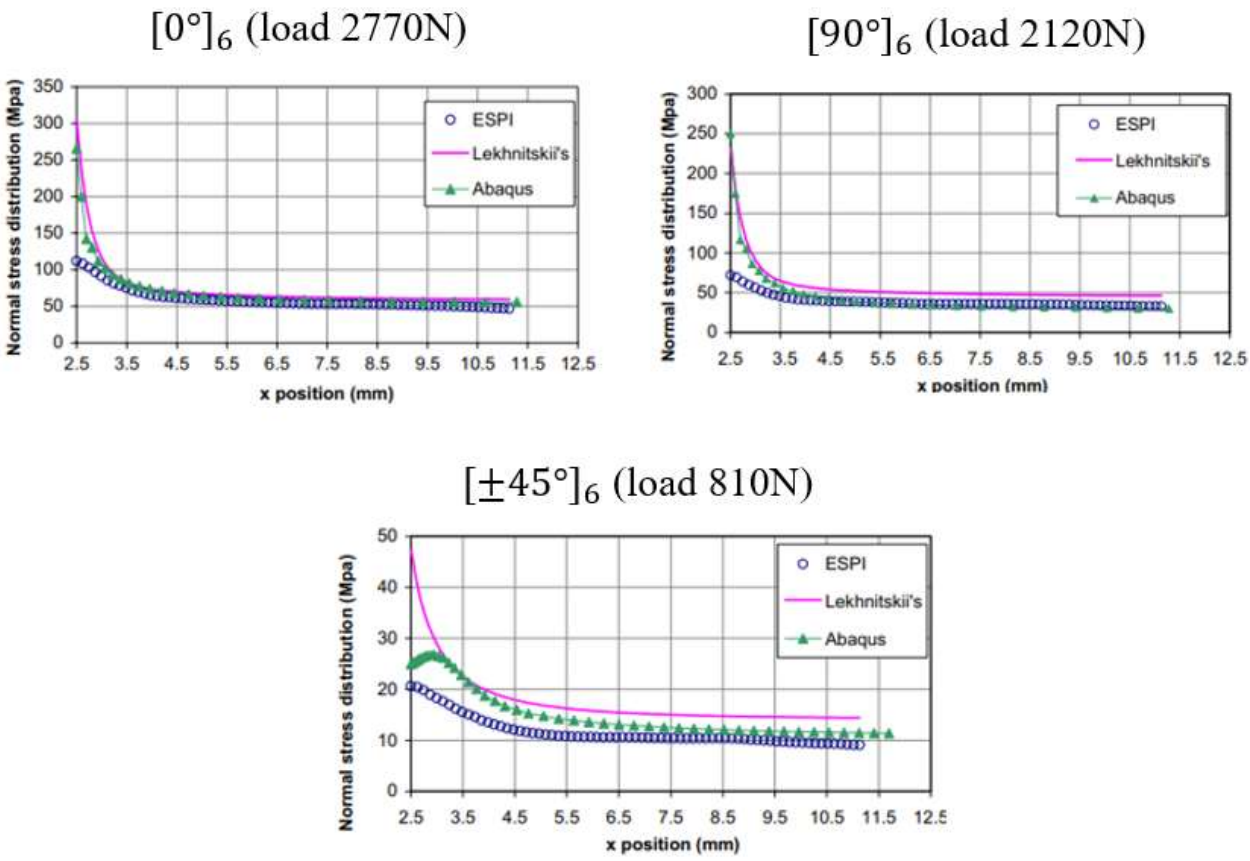

Figure 2-9: Stress distribution of a woven fabric composite subject to a tensile load [21]

Khechai et al. [22] conducted an analysis of stress and strength degradation in notched composite plates using the DIC technique. It was shown that the DIC method provides accurate information to help identify the possible damage zones and the stress distribution. The PSC was also used as well as a finite element model to calculate the SCFs. The SCF values calculated using analytical, numerical and experimental approaches are tabulated in Table 2.5. Estimates of the SCFs with the PSC and the numerical model are within 17% of the experimental results for fiber orientations of 0º, 45º and -45º. However, a fiber orientation of 90º induces an error of approximately 100% when experimental results are compared to both the analytical and numerical models.

Table 2.5: SCF for plates with different fiber orientation angles under tensile load [22]

SCF for plates with different fiber orientation angles under tensile load.

Materials	Fiber Orientation	Analytical	FEM	Experimental
Aluminum	–	3.000	3.117	3.695
E-Glass/Epoxy	0°	3.939	4.047	4.224
	45°	2.827	2.776	3.184
	−45°	2.827	2.776	3.358
	90°	3.047	3.151	1.655

Khechai [22] also analyzed different types of discontinuities, such as circular and rectangular notches, and demonstrated that the DIC technique provides the capability to generate strain contour plots when encountering different discontinuity shapes. This may be seen in Figure 2-10.

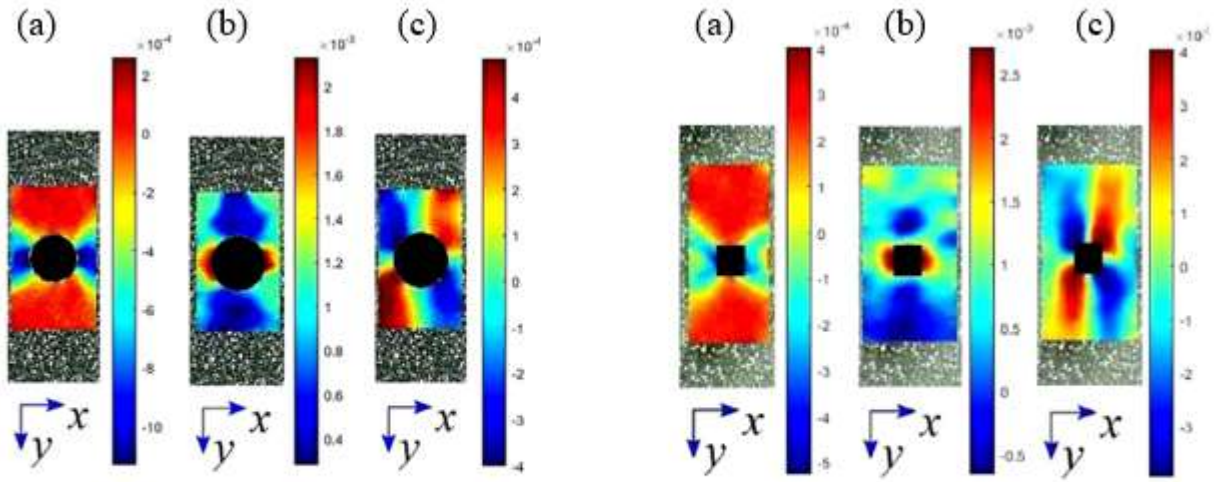

Figure 2-10: DIC engineering strain contour plots [22]

Other works have been done on stress concentration of notched composites using the DIC technique. Duan et al. [23] analyzed the stress concentration at the notch edge of long glass fiber reinforced polypropylene composites utilizing DIC strains. An example of the strain contour plots from this work is seen in Figure 2-11. The DIC method can plot circumferential, radial and shear strains. Duan [23] also used DIC strain values from the notch edge to the free edge of the specimen to present the different effects of hole size on the strain distribution as illustrated in Figure 2-12.

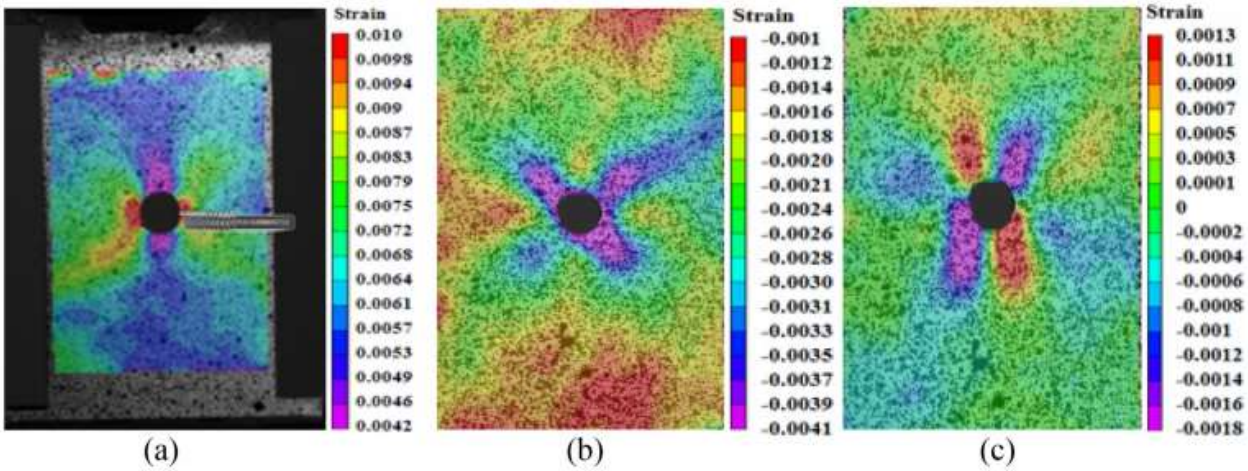

Figure 2-11: The strain distribution including: (a) circumferential strain, (b) radial strain and (c) shear strain [23]

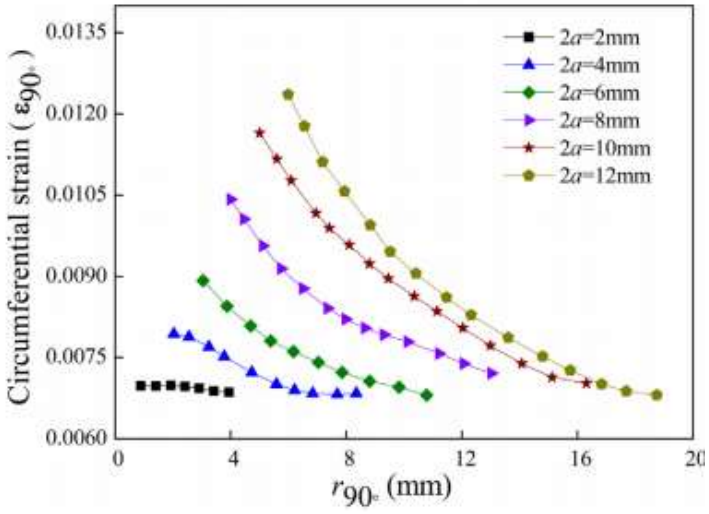

Figure 2-12: Strain variation along sampling path for different hole sizes [23]

A comparison of strain field values of C/SiC notched composite plates calculated using a numerical method (finite element model) and the DIC method was presented in the work of Gao et al. [24]. The strain field contour plots generated by the two methods showed good agreement as seen in Figure 2-13.

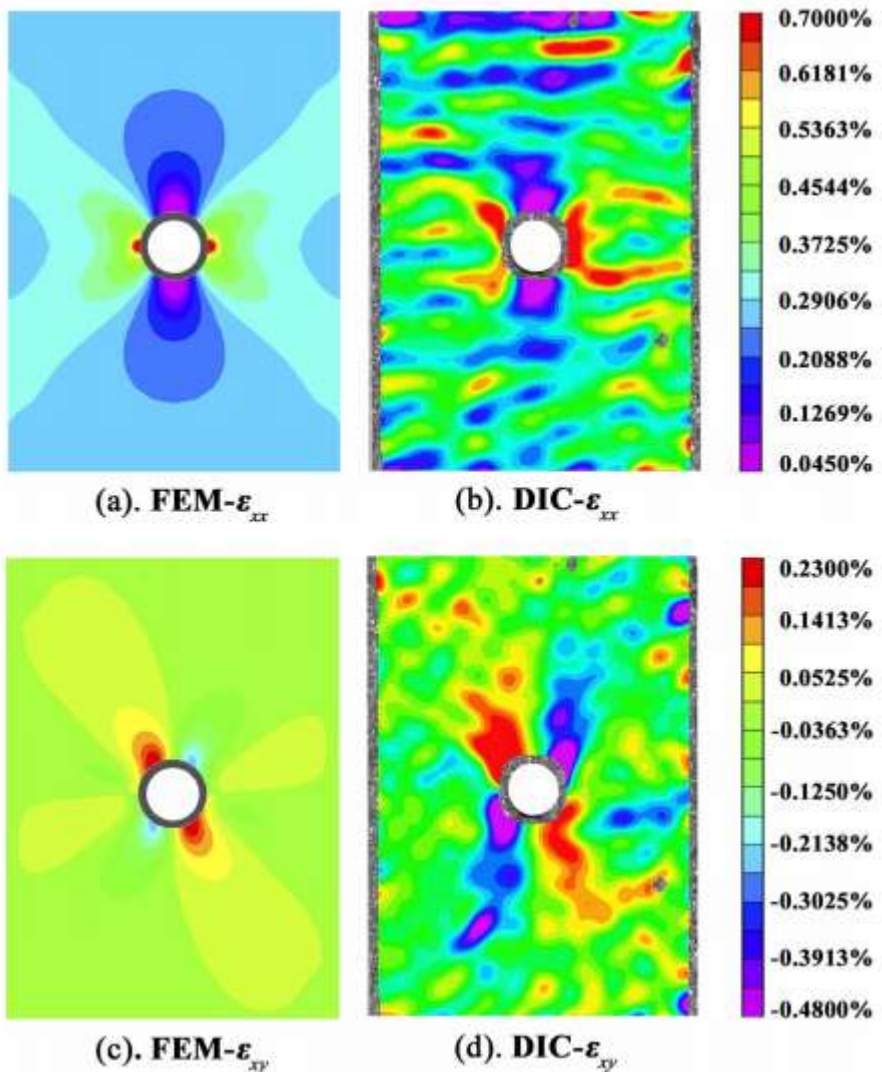

Figure 2-13: Strain field contours of DIC and FEM at a load of 68.88% of UTS [24]

Chawla [25] conducted a numerical study on stress and strain concentration factors (SCNF) in notched composite plates by varying not only hole size but also hole eccentricity. The hole eccentricity (e_y) was considered in the transverse direction of loading as shown in Figure 2-14. The results for SCF and SCNF with respect to varying normalized notch eccentricity is seen in Table 2.6. As the hole eccentricity increases both the SCF and SCNF increase.

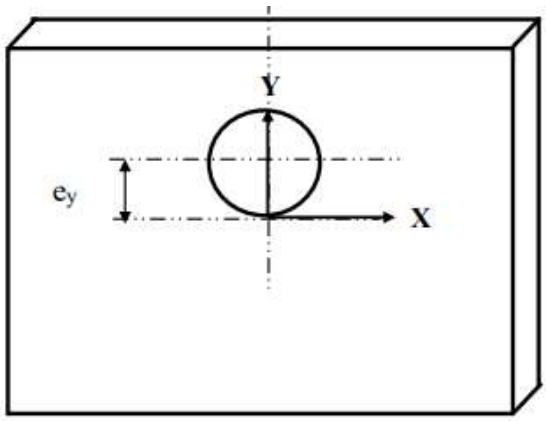

Figure 2-14: Diagram of hole eccentricity with respect to load direction (i.e. x-axis) [25]

Table 2.6: Effect of hole eccentricity on stress and strain concentration factors [25]

Normalized Eccentricity	SCF	SNCF
1	4.06	4.00
1.5	4.20	4.19
2	4.36	4.36
2.5	4.60	4.59
3	4.98	4.97

2.3 Literature Review Key Takeaways

As seen in the literature review, well-defined research has been done on the notched tensile strength and damage progression of cross-ply and quasi-isotropic laminates. However, a reliable prediction whether inclusion of a tightened bolt increases or decreases notch strength is not clear; FHT strength is sometimes higher than OHT strength, but the inverse is true for different conditions.

The PSC and ASC are extensively used in research as well as the application of modified models stemming from both criteria. These criteria have been used to understand the SCFs in notched composite plates and to predict notch strength. The accuracy of the PSC and ASC are dependent on variables which the models do not consider. For example, the thickness of the laminate and the extensive delamination a laminate might undergo prior to failure. These factors most certainly affect the notch strength and stress concentration factors in composites.

The DIC technique is one of the very few methods where strain values near discontinuities in materials can be retrieved. Most of the research conducted on notched composite plates using DIC has been for validation purposes of analytical and numerical models which are used to calculate stress concentration and distribution. To the author's knowledge, few studies were made to investigate and characterize the difference in stress distribution between different composite layups using DIC. Furthermore, the same can be said when analyzing the difference in notch deformation between varying laminates.

CHAPTER 3 METHODOLOGY

The following chapter describes the procedures that were undertaken to:

1) Manufacture and test the open-hole (OHT) and filled-hole (FHT) composite specimens
2) Calculate the experimental stress concentration factors (SCFs) and the stress distribution from the notch edge to the free edge of each specimen using DIC strains
3) Retrieve notch deformation data

3.1 Experimental Procedure

Carbon-fiber laminates reinforced with epoxy are manufactured using the vacuum-assisted resin infusion (VARI) method as seen in Figures 3-1 & 3-2. The laminates are composed of 3K plain-woven carbon fabric with a 193 g/m^2 surface weight and a commercial Araldite epoxy resin system.

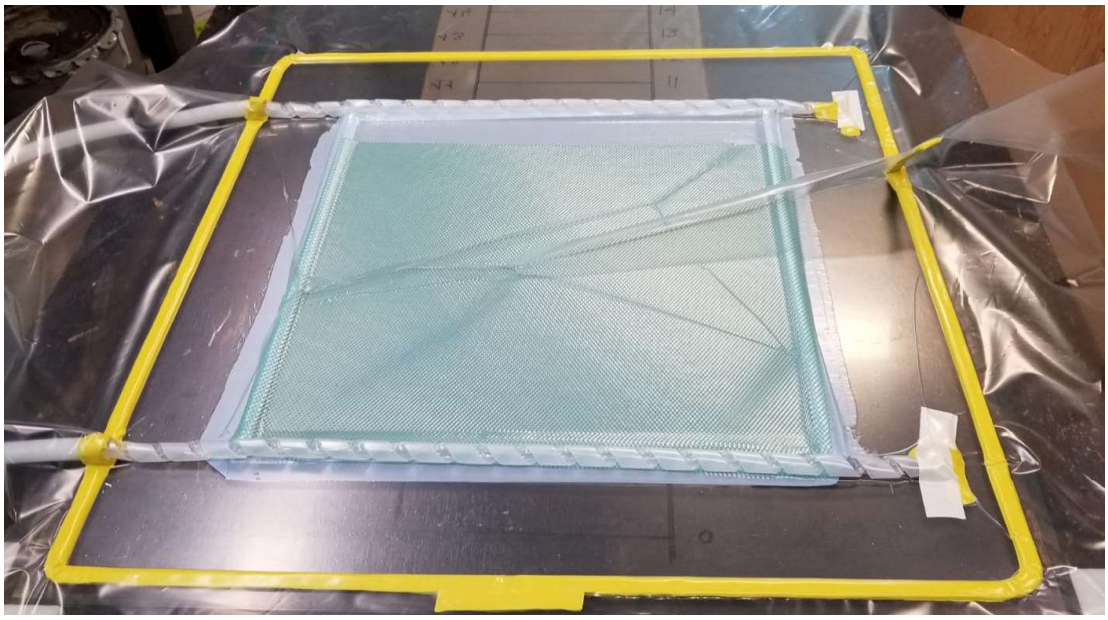

Figure 3-1: Vacuum-assisted resin infusion setup (before resin infusion)

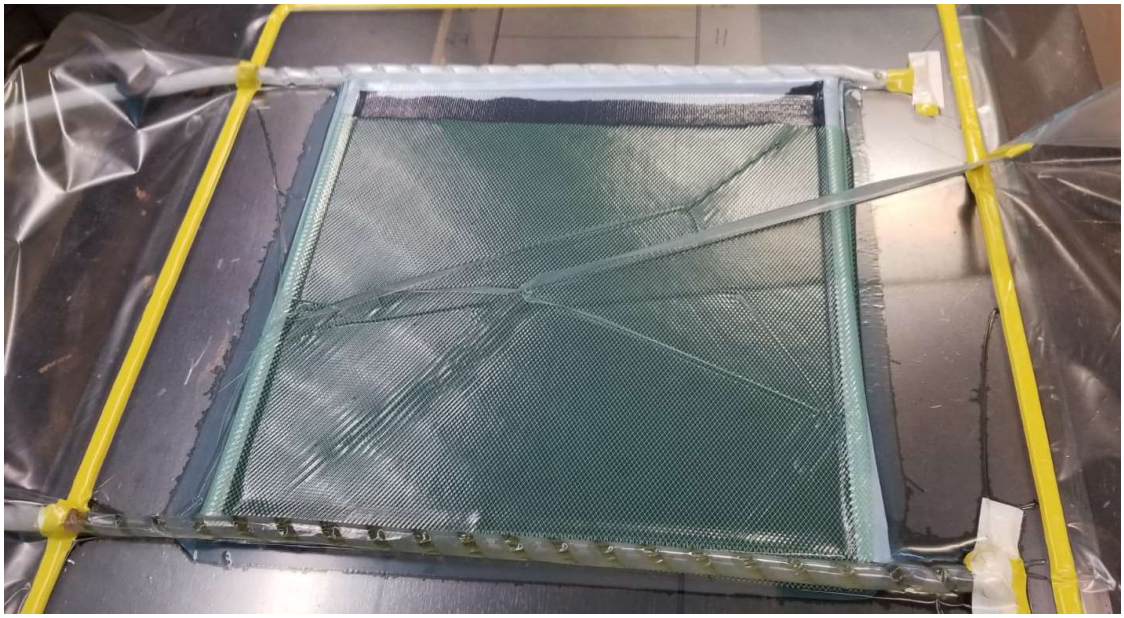

Figure 3-2: Vacuum-assisted resin infusion setup (after resin infusion)

Four different types of specimens were manufactured for this study. The different laminates with their associated stacking sequences and average thicknesses are shown in Table 3.1. The dimensions of the open- and filled-hole specimens are illustrated in Figure 3-3.

Table 3.1: Laminate configurations and thickness

Configuration	Stacking Sequence	Average Thickness
Cross-ply 8-layers	$[(0/90)/(0/90)/(0/90)/(0/90)]_s$	1,66
Quasi-isotropic 8-layers	$[(0/90)/(\pm45)/(0/90)/(\pm45)]_s$	
Cross-ply 12-layers	$[(0/90)/(0/90)/(0/90)/(0/90)/(0/90)/(0/90)]_s$	2,60
Quasi-isotropic 12-layers	$[(0/90)/(\pm45)/(0/90)/(\pm45)/(0/90)/(\pm45)]_s$	

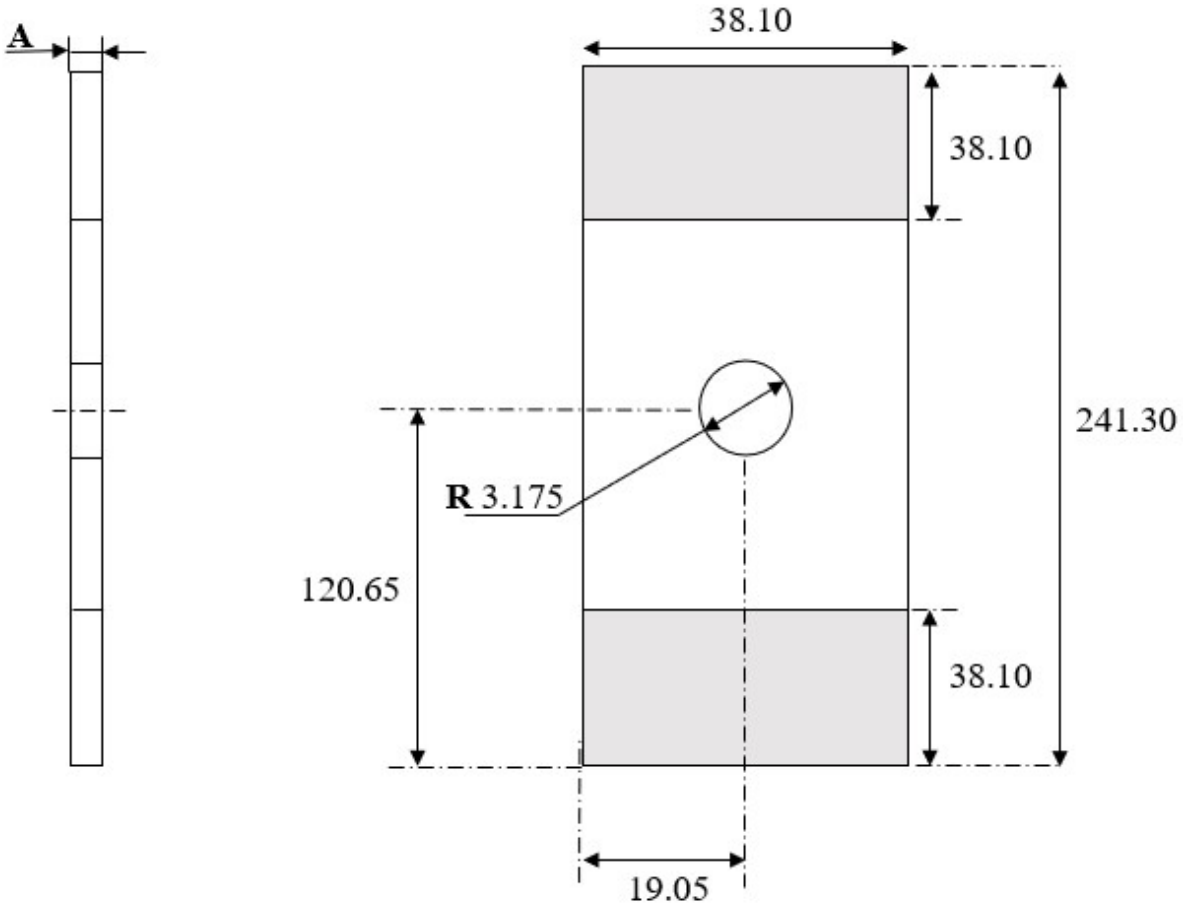

A: 1.66mm thickness for 8-layers and 2.60mm thickness for 12-layers

Figure 3-3: Open-hole and filled-hole specimen dimensions (all dimensions in mm)

Three different tests were conducted:

1. Tensile strength (TS) test (ASTM-D3039)
2. Open-hole tension (OHT) test (ASTM-D5766) with a hole radius of 3.175 mm
3. Filled-hole tension (FHT) test (ASTM-D6742) with a hole radius of 3.175 mm

For each category of tests, five specimens of each configuration were tested, resulting in 60 specimens. The bolts used for the FHT specimens were steel hex head shear bolts (NAS6204-4) with a diameter of 6.35mm. The washers are cadmium-plated steel washers (NAS1149F0463P) with an internal and external diameter of 6.37 mm and 12.70 mm, respectively. All bolts were tightened to a torque of 7 N.m applied with a Tohnichi Dial Torque Wrench (DB25N-S). The

uniaxial tests were conducted on a servo-hydraulic MTS machine model 810. The 810 MTS offers extensive testing capabilities and a load capacity up to 50 kN. It is appropriate for fatigue tests, fracture tests, and monotonic tests.

The DIC technique was used to capture the full-field deformation of the specimen throughout the uniaxial tests. Two Charge Coupled Device (CCD) cameras were used, which are 5-megapixel Pointgrey Grasshopper with pixel size of 3.45 for the camera sensor. A light source to illuminate the specimens was also part of the set up. All specimens were spray painted with white spray paint and then a random speckle pattern was applied as seen in Figure 3-4. The cameras took photos at a rate of 2 frames per second. The captured images were processed using the Correlation Solution software VIC-3D 7 to obtain strain values. An example of the uniaxial test setup with DIC cameras can be seen in Figure 3-5.

Note: Figure 3-5 includes a triple-bolted single lap joint and not an open-hole or filled-hole specimen, however the test setup remains unchanged for all specimens tested.

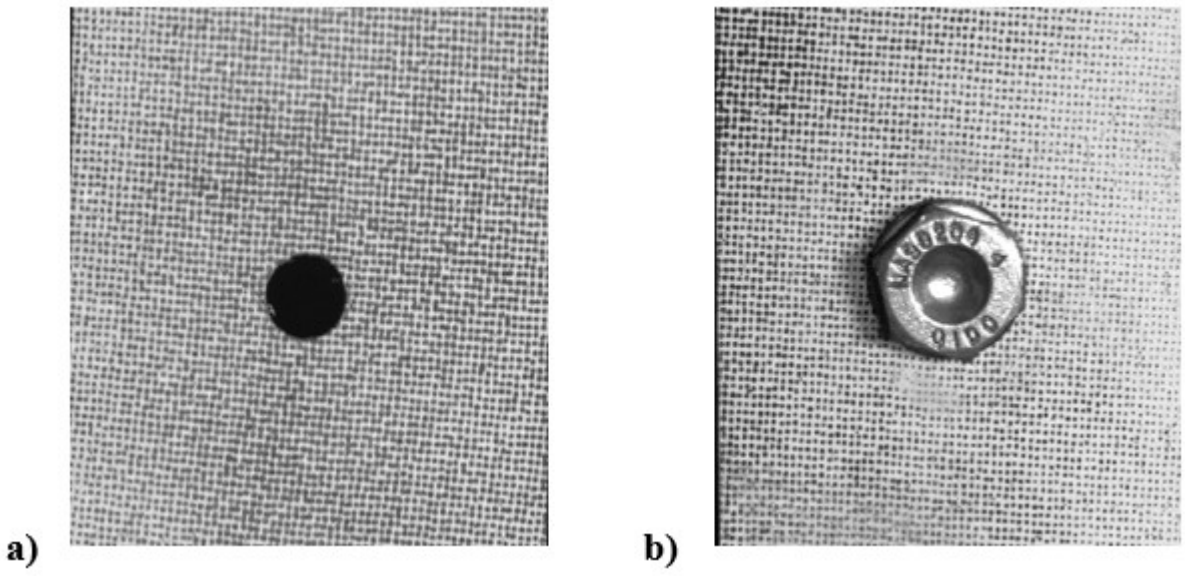

Figure 3-4: DIC speckle patterns a) OHT specimen b) FHT specimen

Figure 3-5: Uniaxial tensile test setup with DIC cameras

3.2 Calculating Stress Distribution and Stress Concentration

Analytical Stress Concentration Factors

As discussed in the literature review, many researchers have altered the classical method of the PSC and ASC. In this investigation however, the classical method proposed by Whitney-Nuismer [9] is used for the following three reasons:

1) Simplicity
    - Depends on two parameters (unnotched strength and characteristic length)
2) Accuracy
    - Generally gives good accuracy when compared to experimental results depending on the laminates investigated
3) Reliability
    - The model has been in use for over three decades

In this research, finite width plates are used and therefore a FWC must be applied as explained in section 2.2.2 within the literature review.

Experimental Stress Distribution

The experimental strains in the x and y direction (ε_{xx} and ε_{yy}) at the notch boundary to the free edge of the specimen were obtained from experimental data using the DIC method as seen in Figure 3-6.

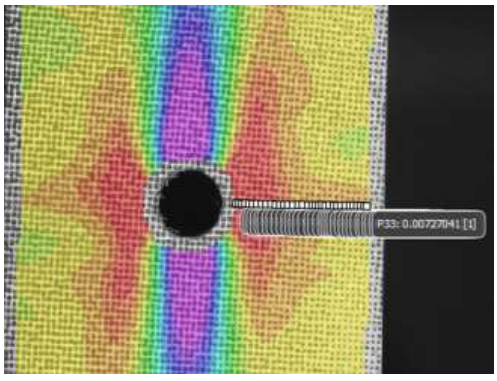

Figure 3-6: Reference points in VIC 3D-7 to obtain strain data

The force per unit length in the normal direction (N_{xx}) of the hole boundary was calculated using the principles of laminate theory according to the following relation:

$$N_{xx} = A_{11}\varepsilon^{\circ}_{xx} + A_{12}\varepsilon^{\circ}_{yy} + A_{16}\gamma^{\circ}_{xy} + B_{11}k_{xx} + B_{11}k_{yy} + B_{16}k_{xy} \tag{3.1}$$

The composite plates investigated are balanced and symmetric, thus the extensional stiffness matrix ($[A]$) and the coupling stiffness matrix ($[B]$) are simplified to:

$$[A] = \begin{bmatrix} A_{11} & A_{12} & 0 \\ A_{21} & A_{22} & 0 \\ 0 & 0 & A_{66} \end{bmatrix} \tag{3.2}$$

And:

$$[B] = 0 \tag{3.3}$$

The normal force per unit length from Equation (3.1) becomes:

$$N_{xx} = A_{11}\varepsilon^{\circ}_{xx} + A_{12}\varepsilon^{\circ}_{yy} \tag{3.4}$$

And the normal stress is found by dividing the normal force per unit length by the thickness of the laminate:

$$\sigma_{xx} = \frac{N_{xx}}{h} \tag{3.5}$$

Where:

- h is the specimen thickness

The experimental stress concentration factor is calculated using the following relation:

$$K^{EXP}_{\frac{\pi}{2}} = \frac{\sigma_{TS}}{\sigma_{OHT}} \tag{3.6}$$

Where:

- σ_{TS} is the tensile strength of the unnotched specimen (TS)

- σ_{OHT} is the tensile strength of the notched specimen (OHT)

The extension stiffness matrix $[A]$ for each laminate investigated is given below:

Cross-ply 8 layers (CP8)

$$[A] = \begin{bmatrix} 101{,}67 & 1{,}93 & 0 \\ 1{,}93 & 101{,}67 & 0 \\ 0 & 0 & 2{,}60 \end{bmatrix} \times 10^9 \frac{N}{mm}$$

Cross-ply 12 layers (CP12)

$$[A] = \begin{bmatrix} 162{,}46 & 3{,}07 & 0 \\ 3{,}07 & 162{,}46 & 0 \\ 0 & 0 & 4{,}16 \end{bmatrix} \times 10^9 \frac{N}{mm}$$

Quasi-isotropic 8 layers (QI8)

$$[A] = \begin{bmatrix} 77{,}77 & 25{,}48 & 0 \\ 25{,}48 & 77{,}7 & 0 \\ 0 & 0 & 26{,}15 \end{bmatrix} \times 10^9 \frac{N}{mm}$$

Quasi-isotropic 12 layers (QI12)

$$[A] = \begin{bmatrix} 122{,}41 & 40{,}1 & 0 \\ 40{,}1 & 122{,}41 & 0 \\ 0 & 0 & 41{,}16 \end{bmatrix} \times 10^9 \frac{N}{mm}$$

3.3 Notch Deformation Data Retrieval

Notch deformation analysis of the OHT and FHT specimens was conducted by measuring the longitudinal hole elongation (LHE) and the transversal hole compression (THC) as the applied tensile load was increased until laminate failure occurred. The measurements of the LHE and THC were completed by applying two virtual extensometers (VE); one in the longitudinal (axial) direction and the other in the transversal direction within VIC-3D 7, as seen in Figure 3-7.

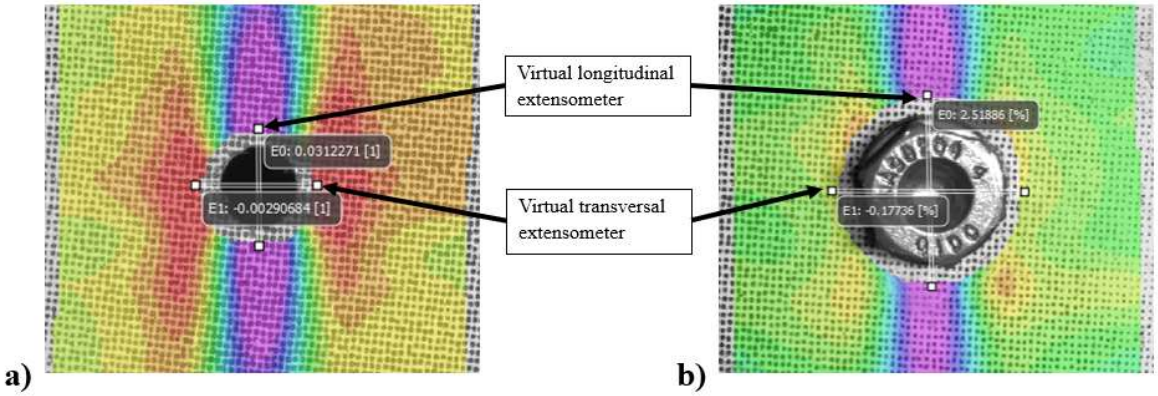

Figure 3-7: Application of virtual extensometers in VIC-3D a) OHT b) FHT

CHAPTER 4 RESULTS AND DISCUSSION

An overview of the tensile strength of the TS, OHT and FHT specimens for the layups investigated will be discussed, followed by presentation of the experimental stress distribution results calculated from DIC strains. The chapter ends with an analysis and discussion of the calculated experimental and analytical stress concentration factors in conjunction with the notch deformation results.

4.1 Open- and Filled-Hole Tensile Strength

The unnotched (TS), notched (OHT) and filled-hole (FHT) average tensile strengths of cross-ply 8-layer (CP8), cross-ply 12-layer (CP12), quasi-isotropic 8-layer (QI8) and quasi-isotropic 12-layer (QI12) laminates are shown in Figure 4-1.

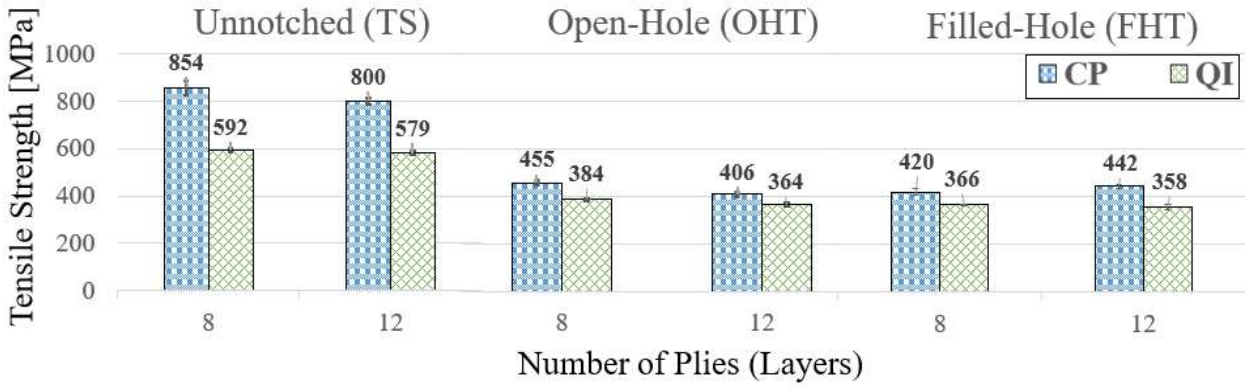

Figure 4-1: Average tensile strength of unnotched (TS), open-hole (OHT) and filled-hole (FHT) of cross-ply and quasi-isotropic 8- and 12-layer laminates

The TS specimens have a greater variance in tensile strength between different layups of the same thickness. For example, the difference in the TS tensile strength between CP8 & QI8 and that of CP12 & QI12 are 44% and 38%, respectively. Whereas, the difference in the OHT strength of the above-mentioned comparisons are 18% and 11%, respectively. Whitney & Kim [26] found that the unnotched tensile strength is much more sensitive to the stacking sequence than the notched tensile strength. However, the method chosen to thicken the laminate has a direct effect on the sensitivity of the notched tensile strength. Green, Wisnom and Hallet [1] found that increasing laminate thickness through ply-level scaling has a greater impact on the notched tensile strength than

increasing laminate thickness through sub-laminate-level scaling. Ply-level scaling is referred to as increasing the number of plies of the same orientation blocked together. Sub-laminate-level scaling is the act of increasing the number of sub-laminates. The thickening method used in this investigation is sub-laminate-level scaling. As seen in Figure 4-1, the FHT specimens all have lower tensile strength than their OHT counterparts, except for CP12. However, the variance in tensile strength is slight and it can therefore be concluded that filling a notch with a clamped bolt does not greatly reduce or increase the tensile strength compared to OHT specimens. Figure 4-2 contains the stress-strain curves of OHT and FHT specimens.

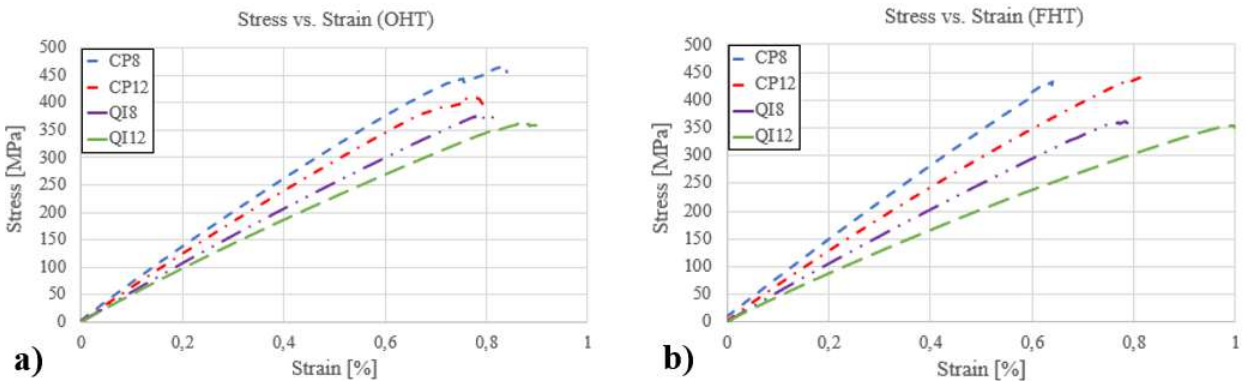

Figure 4-2: Stress-strain and force-strain curves of open- and filled-hole laminates a) OHT stress-strain b) FHT stress-strain

From Figure 4-1 and Figure 4-2 the following observations can be made:

- Cross-ply laminates have higher unnotched, open- and filled-hole tensile strengths than quasi-isotropic laminates. This is due to the increased number of 0^0 plies in CP layups which are in the direction of the applied load.
- The notch tensile strength is affected, but not significantly, by the addition of a clamped bolt. The lower tensile strength of FHT specimens compared to OHT may be explained by the fact that the bolt reduces the amount of damage the notch exhibits. For this reason, the stress concentration cannot be relieved at the notch boundary, leading to a lower tensile strength. CP12 acts as an outlier as its FHT strength is higher than its associated OHT strength.

- Increasing the thickness of a laminate reduces the tensile strength in OHT specimens. Green [1] noted that using sub laminate thickening (which is the laminate thickening method used in this research) disperses the 0^{o} plies uniformly through the thickness of the laminate. This aids in halting the propagation of sub-critical damage, which therefore decreases as laminate thickness increases. This causes a lack of stress relief away from the notch and thus the tensile strength decreases. However, this does not hold true for FHT CP12 laminates; their tensile strength is greater than FHT CP8. As well, the OHT strength of CP12 is less than that of FHT CP12, which goes against the trend in the rest of the laminates investigated. To the author's knowledge there is no clear explanation why CP12 is an outlier. As stated by Gamdani [5], the OHT strength is usually higher than FHT strength, however the inverse may occur. The dependence of the results of OHT and FHT tests on the material characteristics of the laminate are not yet well established. It has also been stated that the effect of the presence of a tightened bolt on the tensile strength of laminates that are not damage-prone may be negligible [6]. Considering the fact that thicker CP laminates are less prone to damage than thinner CP laminates (as mentioned above), it appears that introducing a clamped bolt may not adversely affect the strength.
- Thicker OHT and FHT laminates are stiffer than their thinner counterparts.
- Filling the notch with a clamped bolt has a stiffening effect on the CP8 and QI12 laminates. This can be seen by comparing Figure 4-2 a) and b): OHT CP8 is less stiff than FHT CP8 and the same is seen for QI12. This may be due to the bolt delaying the deformation of the notch, which results in an increased stiffening effect. These results compare well with those presented in Gamdani's research [5].

4.2 Stress Distribution from the Notch Edge to the Free Edge

For validation purposes, a comparison between the stress distribution in notched composite plates calculated using Lekhnitskii's analytical stress model (Equation 2.1) [7] and the experimental stress obtained using DIC strains (Equations 3.4 and 3.5) is shown in Figure 4-3. Note that the finite width correction factor (Y) was applied to the analytical stresses. The FWC in this investigation is equal to 0.98 (Y = 0.98) or 98%. (i.e., a 2% correction was applied to the analytical stresses when used for a finite width plate). Analytical and experimental stress values differ greatly in the region located near the notch edge due to the high strain gradient in this zone, which induces damage and

redistributes the stress away from the notch. This is well presented in the DIC strain contour plots (Figure 4-4); the strain in the axial direction (direction of the applied load) changes drastically just a few millimeters from the notch for each configuration. The analytical model does not take this phenomenon into account. Further away from the notch however, the experimental and analytical stresses converge since high strain gradients are not present. It is important to note that the DIC cannot capture the difference in stress values near the notch boundary for FHT specimens since the washer and the bolt head cover more than 4 mm of the notch boundary.

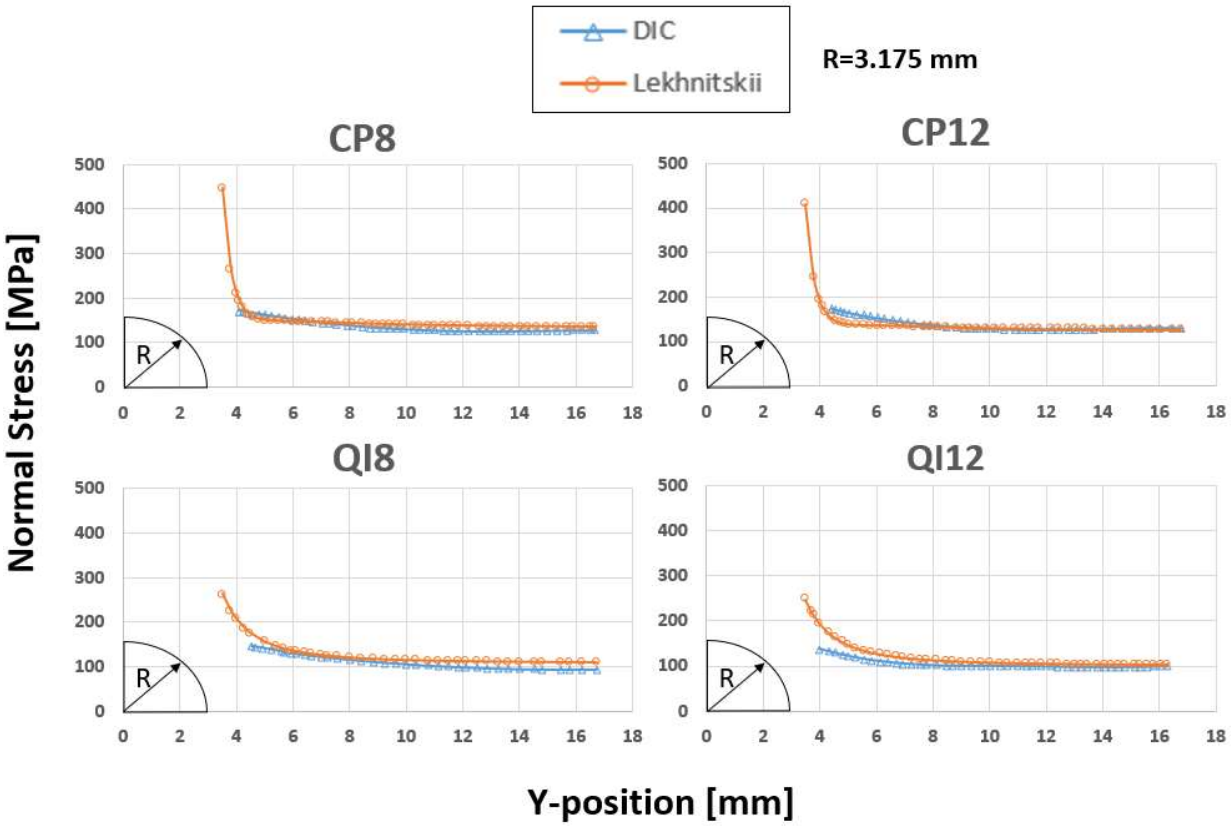

Figure 4-3: Analytical vs. experimental normal stress near the notch boundary to the free edge of the specimen at 25% max load for cross-ply 8 & 12 layer and quasi-isotropic 8 & 12 layer OHT specimens

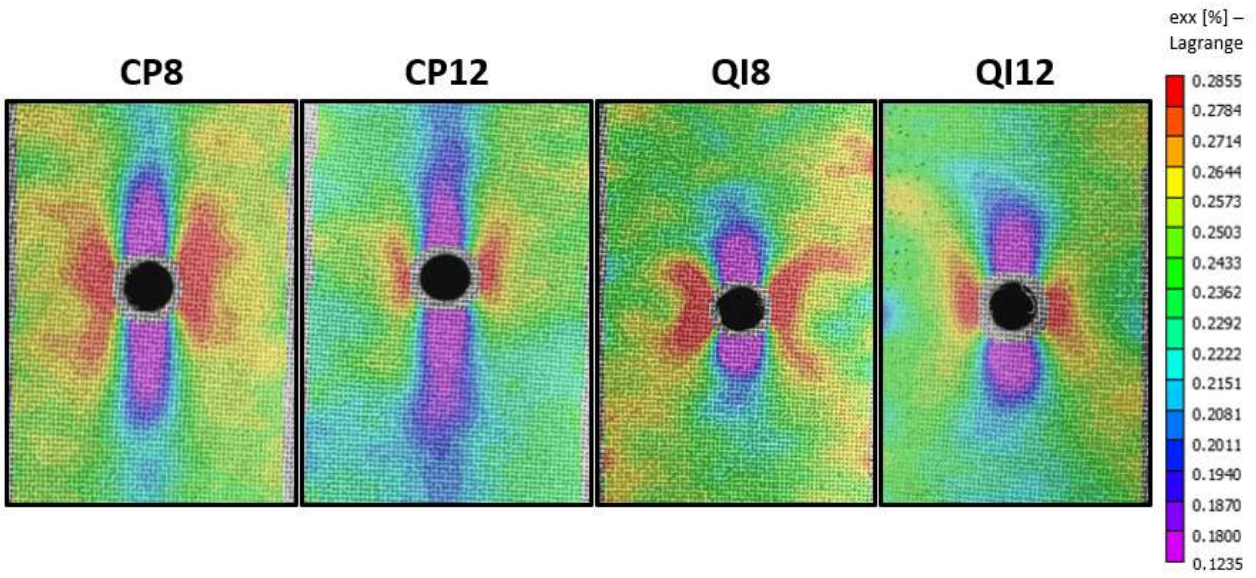

Figure 4-4: Strain plots in the axial direction (ε_{xx} [%]) at 25% max load for OHT cross-ply and quasi-isotropic 8- & 12- layer laminates

A comparison of the normalized stress distribution of DIC measurements from the notch boundary to the free edge of the specimen for CP8, CP12, QI8 and QI12 laminates at 95% of their maximum applied load, is shown in Figure 4-5. A good indication of the stress distribution capability of a laminate is obtained by subtracting the free edge normalized stress from the normalized stress near the notch boundary. This is called the stress gradient at 95% of the maximum applied load as seen in Equations (4.1) and (4.2) below:

$$\Delta_{OHT/TS} = \frac{OHT}{TS}_{Notch} - \frac{OHT}{TS}_{Free} \tag{4.1}$$

$$\Delta_{FHT/TS} = \frac{FHT}{TS}_{Notch} - \frac{FHT}{TS}_{Free} \tag{4.2}$$

A laminate with a smaller normalized stress gradient can be said to have a better capability for distribution of stress. It is important to note that a high normalized stress value indicates that the laminate is less sensitive to the inclusion of a notch than a laminate with a low normalized stress

value. Therefore, the lower the curve is positioned on the y-axis, the more sensitive that laminate is to the presence of a notch.

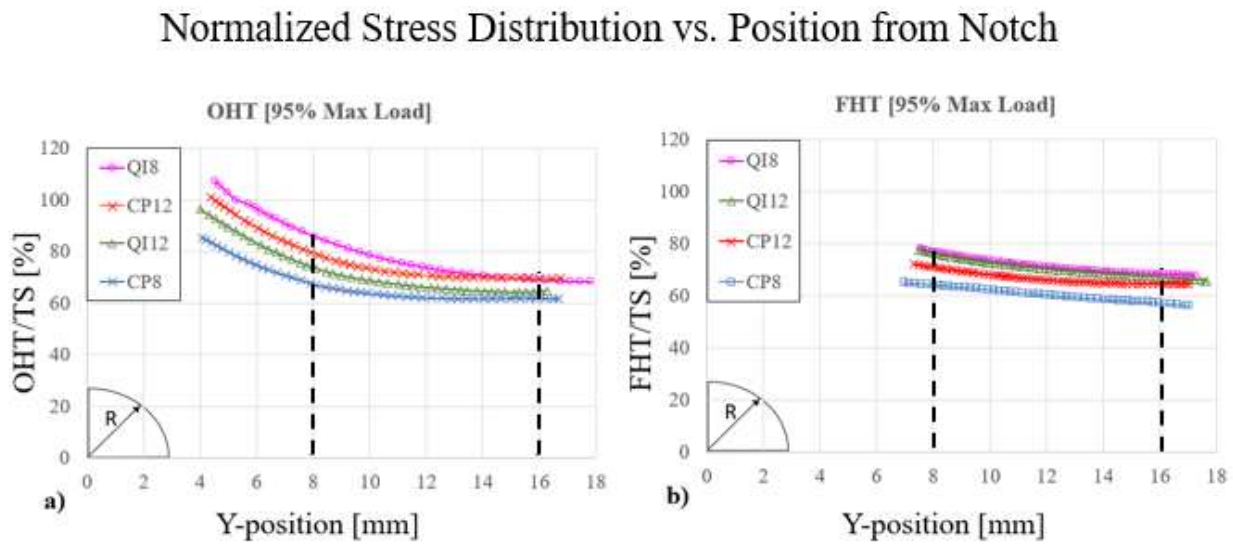

Figure 4-5: DIC normalized stress distribution from the notch edge to the free edge of open- and filled-hole specimens a) OHT at 95% max load b) FHT at 95% max load

One of the limitations of the DIC technique is that strains can only be mapped starting ~2mm away from the notch edge. As seen in Figure 4-6 to Figure 4-9 there are no mapped strain values around the circumference of the hole. When adding a clamped bolt with a washer, the distance between the notch boundary and the start of the DIC strain values increases to ~5mm. Therefore, to compare OHT and FHT stress distribution capabilities, normalized stress values between 8mm and 16mm from the center of the notch are used, as seen in Figure 4-5 by the black dashed lines. The results of the normalized stress gradients for each configuration are presented in Table 4.1 for OHT and FHT specimens.

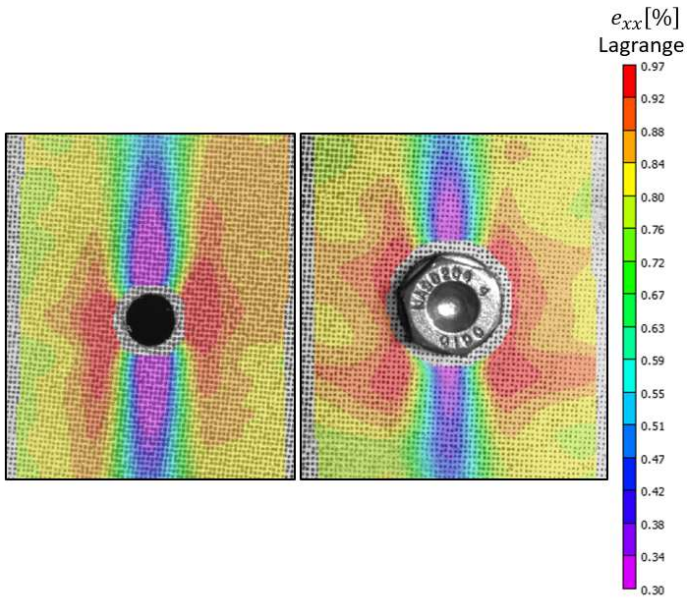

Figure 4-6: Strain contour plots in the axial direction (ε_{xx} [%]) at 95% of the maximum load (ML) for cross-ply open- and filled-hole 8 layer laminates (CP8)

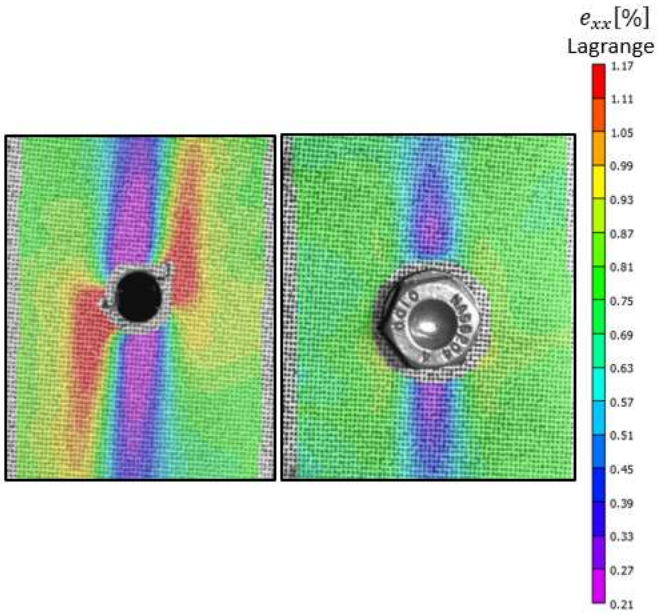

Figure 4-7: Strain contour plots in the axial direction (ε_{xx} [%]) at 95% of the maximum load (ML) for cross-ply open- and filled-hole 12 layer laminates (CP12)

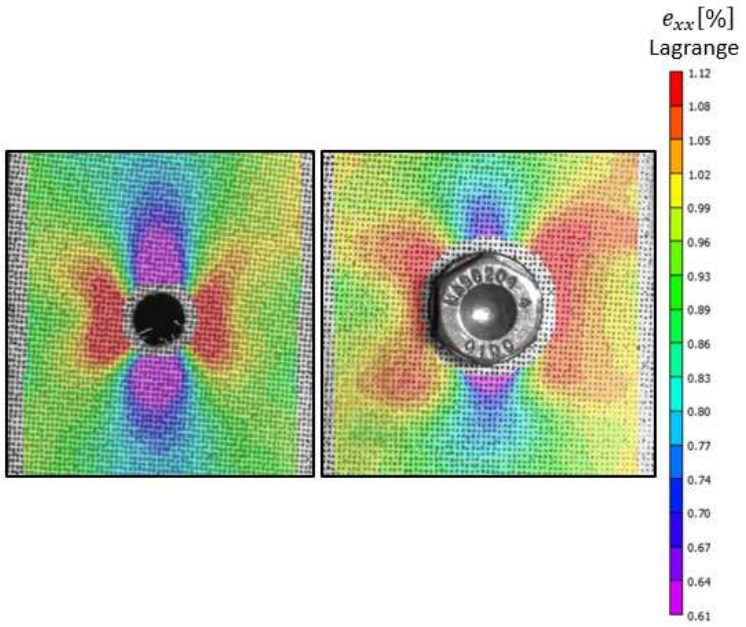

Figure 4-8: Strain contour plots in the axial direction (ε_{xx} [%]) at 95% of the maximum load (ML) for quasi-isotropic open- and filled-hole 8 layer laminates (QI8)

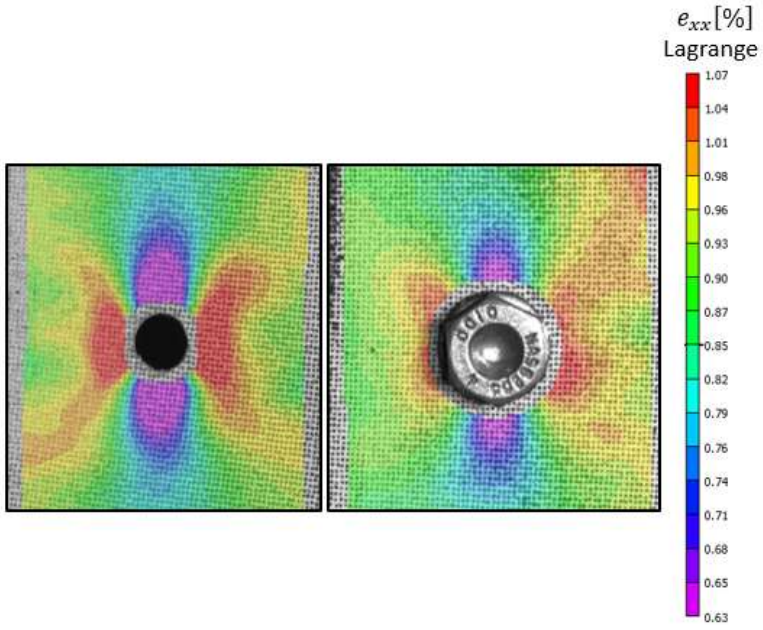

Figure 4-9: Strain contour plots in the axial direction (ε_{xx} [%]) at 95% of the maximum load (ML) for quasi-isotropic open- and filled-hole 12 layer laminates (QI12)

Table 4.1: Stress gradient between 8mm and 16mm from the center of the notch for OHT and FHT specimens at 95% maximum load

	OHT			FHT			OHT vs. FHT
	$\frac{OHT}{TS}_{Notch}$ [%]	$\frac{OHT}{TS}_{Free}$ [%]	$\Delta_{\frac{OHT}{TS}}$ [%]	$\frac{FHT}{TS}_{Notch}$ [%]	$\frac{FHT}{TS}_{Free}$ [%]	$\Delta_{\frac{FHT}{TS}}$ [%]	$\Delta_{95\%}$ [%]
CP8	67	62	5	64	57	7	40
CP12	80	70	10	71	64	6	-40
QI8	86	69	17	77	68	9	-47
QI12	73	65	9	76	67	9	0

The stress distribution capabilities ($\Delta_{OHT/TS}$ and $\Delta_{FHT/TS}$) of OHT laminates are quite scattered. The OHT laminate with the greatest stress distribution capability is CP8 with a normalized stress gradient of 5%. The laminate with the worst distribution capability is QI8 with a normalized stress gradient of 17%. The remaining laminates, CP12 and QI12, fall in-between and their stress distribution capabilities are approximately identical with a 10% and 9% normalized stress gradient, respectively. The fact that CP8 has a better stress distribution capability than CP12, further proves that thickening the laminate decreases its tensile strength, as previously mentioned in Section 4.1. If the thinner cross-ply laminate has more sub-critical damage, the stress gets re-distributed away from the notch, which acts as a stress reliever. This leads to a higher tensile strength compared to a thicker laminate of the same lay-up. Thinner OHT CP laminates are therefore better at distributing stress away from the boundary of the notch than their thicker counterparts. However, the inverse is true for QI layups; thicker OHT QI laminates distribute stress better than their thinner counterparts. One would expect QI layups to follow the same trend as CP layups in stress distribution since thicker laminates exhibit less damage due to the increased number of dispersed 0^{o} layers, which aids in arresting damage propagation through the thickness. A theoretical explanation may be found by studying the types of damage exhibited in both layups. CP layups are known to exhibit axial splits in the vicinity of the notch in the 0^{o} plies, which are then followed by matrix cracking in the 90^{o} plies. Note that this matrix cracking in the 90^{o} plies occurs on the outside of the axial splitting [2]. This is because the axial splits in the 0^{o} plies cut off the stress concentration at the notch edge. QI layups do not typically exhibit axial splits and instead are seen to have $\pm 45^{o}$

and 90º plie matrix cracking. This difference in damage mechanisms may influence the stress distribution capabilities of layups with varying thicknesses.

The stress distribution capabilities of FHT laminates are quite different when compared to those of OHT laminates. By adding a clamped bolt into the notch, the stress distribution capabilities of each laminate become less scattered and are fairly similar. The FHT laminates with the greatest stress distribution capabilities are CP8 and CP12 with normalized stress gradients approximately identical at 7% and 6%, respectively. The QI8 and QI12 laminates follow right behind with identical normalized stress gradients of 9%. Considering that the difference between the highest and lowest stress gradient among the laminates investigated is only 3% (i.e., they have approximately identical stress distribution capabilities), it can be concluded that the clamped bolt nullifies any benefits the laminate thickness or layup may have on the stress distribution capability when compared to OHT specimens.

It is worth noting that the stress distribution capability is identical between OHT and FHT for the QI12 laminate. However, when the bolt is introduced into the QI8 laminate, the stress distribution capability is reduced by 47%. The addition of the bolt does not affect the stress distribution capability of the thicker quasi-isotropic laminate but greatly affects that of the thinner one.

4.3 Stress Concentration Factors and Notch Deformation

4.3.1 Stress Concentration Factors

The characteristic lengths and the predicted strength of the OHT and FHT laminates according to the PSC and ASC are presented in Table 4.2. Values of the experimental stress concentration factors (SCF) as well as those calculated using the PSC and ASC are shown in Table 4.3. It demonstrates that the PSC provides outstanding accuracy for the laminate configurations investigated for OHT and FHT specimens. The greatest difference between the experimental and PSC SCFs is present in the OHT CP12 laminate, but this difference is only 4%. The SCFs calculated with the PSC are even more accurate when applied to FHT specimens; all margins of error drop below 3%.

The ASC has a greater margin of error when compared to the experimental SCFs for cross-ply laminates with a difference of 10% and 13% for CP8 and CP12 OHT specimens and a difference of 15% and 7% for FHT specimens, respectively. However, the accuracy of the ASC SCFs is

excellent when used for QI8 and QI12 laminates (a difference of less than 1% compared to the experimental results). It is not exactly clear to the author why the ASC induces such a great error when calculating the predicted strength and SCFs for cross-ply layups in this investigation. However, Green [1] stated that the ASC is not accurate for laminates that exhibit extensive delamination. The ASC assumes that the strength of the specimen is dependent only on hole size and is independent of laminate thickness. When laminates exhibit widespread delamination then the failure strength is dependent on the thickness, and therefore the ASC may produce erroneous results. But delamination can be exhibited by both cross-ply and quasi-isotropic layups as shown by O'Higgins [2]. Therefore, it cannot be concluded with certainty that delamination is the cause of the inaccuracies of the ASC for CP laminates.

Table 4.2: Open- and filled-hole strength predictions and characteristic lengths according to the PSC and ASC

	Experimental		**PSC**					**ASC**				
	Strength OHT [MPa]	Strength FHT [MPa]	d_0 [mm]	Strength Prediction OHT [MPa]	Strength Prediction FHT [MPa]	Error OHT [%]	Error FHT [%]	a_0 [mm]	Strength Prediction OHT [MPa]	Strength Prediction FHT [MPa]	Error OHT [%]	Error FHT [%]
CP8	455	420	0,65	443	416	-2,6	-1,0	2,60	505	496	11,0	18,1
CP12	406	442	0,60	390	440	-3,9	-0,5	2,40	469	479	15,5	8,4
QI8	384	366	1,49	381	369	-0,8	0,8	4,57	387	367	0,8	0,3
QI12	364	358	1,36	360	360	-1,1	0,6	4,04	367	359	0,8	0,3

Table 4.3: Open- and filled-hole experimental stress, PSC and ASC concentration factors

	Experimental		**PSC**				**ASC**			
	$K_{\pi/2}^{EXP}$ OHT	$K_{\pi/2}^{EXP}$ FHT	$K_{\pi/2}^{PSC}$ OHT	$K_{\pi/2}^{PSC}$ FHT	Error OHT [%]	Error FHT [%]	$K_{\pi/2}^{ASC}$ OHT	$K_{\pi/2}^{ASC}$ FHT	Error OHT [%]	Error FHT [%]
CP8	1,88	2,03	1,93	2,05	2,7	1,0	1,69	1,72	-10,1	-15,3
CP12	1,97	1,81	2,05	1,82	4,1	0,6	1,71	1,67	-13,2	-7,7
QI8	1,54	1,62	1,55	1,61	0,6	-0,6	1,53	1,61	-0,6	-0,6
QI12	1,59	1,62	1,61	1,61	1,3	-0,6	1,58	1,61	-0,6	-0,6

It is interesting to note that the PSC overestimates the SCFs, whereas the ASC underestimates the SCFs when compared to the experimental results.

Ray-Chaudhuri and Chawla's [25] investigation into the stress and strain concentration factors of carbon and glass fiber reinforced polymers showed that the SCF of flat plates are independent of the number of plies in a laminate. This is due to the lack of curvature, which implies that the laminate should have the same state of stress at any given point. According to observations made during this investigation however, this does not hold true. From Table 4.3, thinner OHT laminates have a smaller SCF than their counterparts because thinner laminates exhibit more damage due to the decreased number of 0^{o} plies.

Thinner FHT specimens (CP8 and QI8) present an approximate 5% increase in their SCFs compared to OHT specimens. This is due to the clamping load that retains the integrity of the notch and does not allow the same stress relief at the notch boundary as seen in OHT specimens. The SCF of thicker laminates (CP12 and QI12) are not as affected by the inclusion of a tightened bolt; the SCF of CP12 FHT is lower than that of its OHT and the difference in SCF values for QI12 OHT and FHT is negligible. This may be because thinner laminates are more adversely affected by damage then their thicker counterparts.

4.3.2 Notch Deformation

The LHE and THC plotted against the normalized stress (OHT/TS and FHT/TS) of OHT and FHT specimens for each laminate are illustrated in Figure 4-10. The global longitudinal elongation (GLE), which can also be considered as the total elongation the specimen undergoes, is plotted against the normalized stress of OHT and FHT in Figure 4-11. It is well-known that cross-ply laminates are more rigid in nature than quasi-isotropic laminates, therefore the GLE of a cross-ply laminate under uniaxial tension up until failure should be less than that of a quasi-isotropic laminate. However, the LHE of cross-ply laminates are greater than quasi-isotropic laminates while their GLE is less. The GLE and LHE at 40% of OHT/TS and FHT/TS are shown in Table 4.4. Note that 40% of the normalized stress is used as a reference point; any percentage of normalized stress will show the same trend.

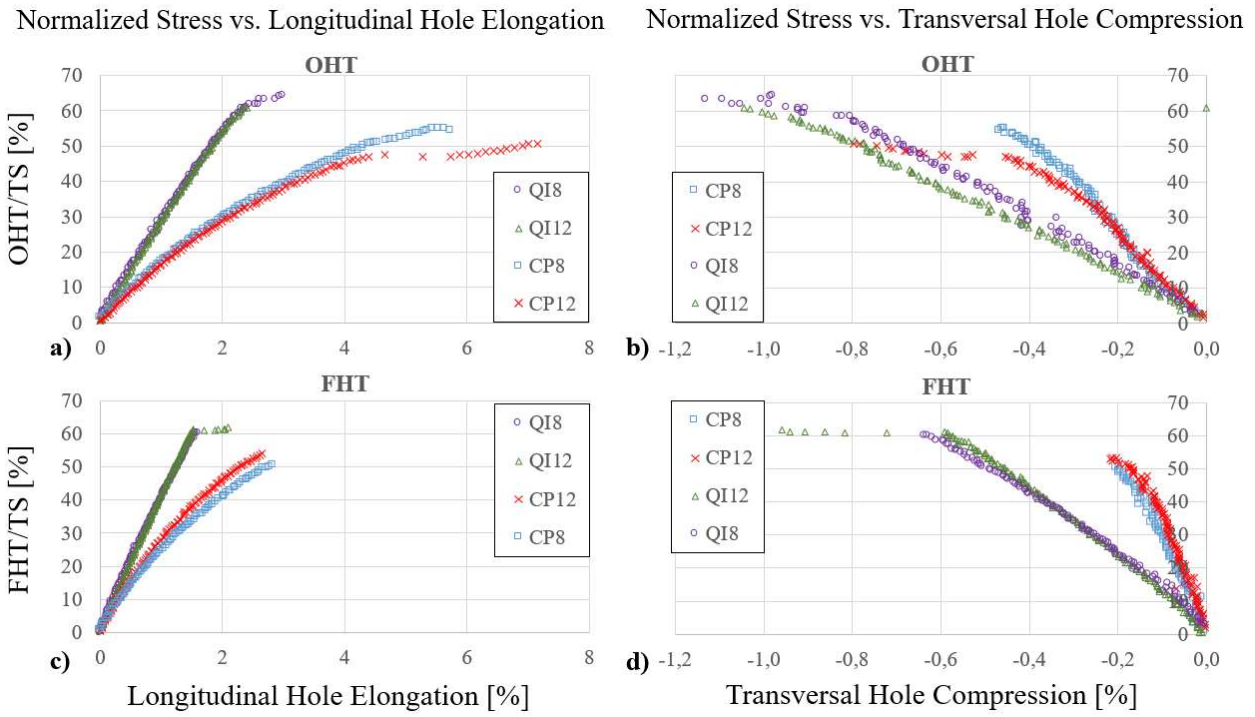

Figure 4-10: The effect of laminate layup on open- and filled-hole notch deformation a) OHT - longitudinal hole elongation b) OHT - transversal hole compression c) FHT - longitudinal hole elongation d) FHT - transversal hole compression

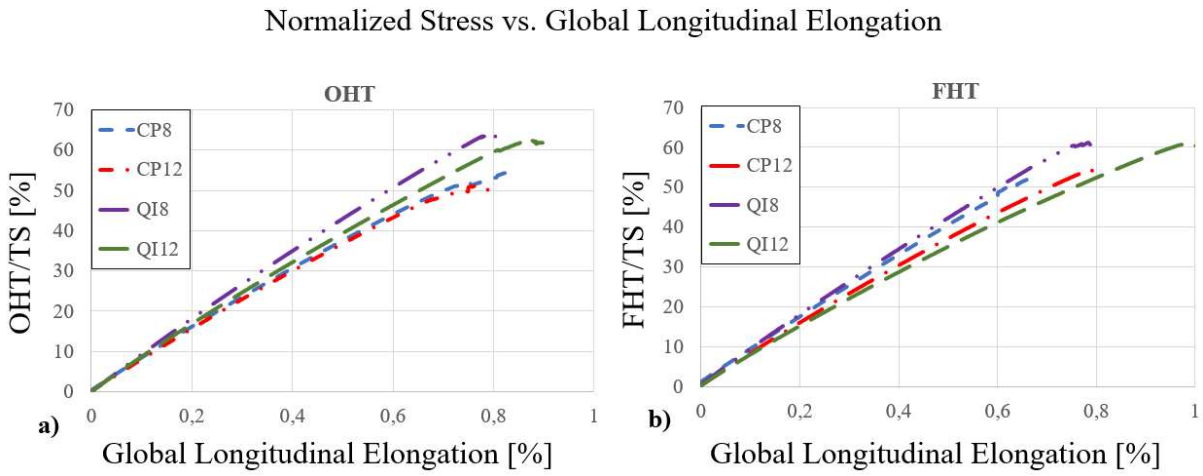

Figure 4-11: Normalized stress vs. global longitudinal elongation a) OHT - global longitudinal elongation b) FHT - global longitudinal elongation

Table 4.4: Global longitudinal elongation and local hole elongation of open- and filled-hole laminates at 40% OHT/TS & FHT/TS

40% OHT/TS & FHT/TS						
	OHT			FHT		
	GLE [%]	LHE [%]	ΔStrain [%]	GLE [%]	LHE [%]	ΔStrain [%]
CP8	0,53	3,12	489	0,49	1,95	298
CP12	0,55	3,27	495	0,54	1,62	200
QI8	0,46	1,43	211	0,47	1,00	113
QI12	0,51	1,42	178	0,57	0,96	68

At 40% of the OHT/TS and FHT/TS, the GLE of all laminates shows very little variation, with the strain values ranging between 0,46% to 0,55%. However, LHE values diverge significantly between different lay-ups. CP8 and CP12 have LHE strains of 3,12% and 3,27% for OHT specimens and 1,95% and 1,62% for FHT specimens, respectively. QI8 and QI12 have LHE strains of 1,43% for OHT and 1% for FHT. Throughout the range of applied tensile load, the longitudinal LHE of cross-ply layups are greater than quasi-isotropic layups (approximately 100% more). The opposite would be expected since cross-ply laminates have higher rigidity than quasi-isotropic laminates. This phenomenon was exhibited in both OHT and FHT specimens. Filling the notch with a clamped bolt greatly reduces the longitudinal and transversal deformation because the bolt upholds the geometric integrity of the hole. O'Higgins [2] found a direct correlation between the amount of damage an OHT laminate sustains prior to failure and its tensile strength. The same correlation is seen here in FHT specimens. Since the notch in the FHT specimens undergoes less deformation, a smaller amount of damage is present at the notch boundary. This results in less stress relief, which explains why the FHT specimens in this investigation have lower tensile strength than the OHT specimens. CP12 is an outlier, as its OHT strength is less than its FHT strength.

A laminate with a greater value of LHE does not imply that it will also have a higher THC when compared to a laminate with a different layup. Consider the example of two isotropic materials, A and B, where A is more rigid than B, both having a centrally located notch and under uniaxial tension. Notch B should have higher LHE and THC values compared to notch A. However, this is

not the case in carbon-fiber composite materials. Cross-ply laminates, which have a large LHE, have a lower THC compared to quasi-isotropic laminates. The notch elongates more in cross-ply than quasi-isotropic, however the cross-ply notch exhibits less transversal compression than the quasi-isotropic notch. This trend is seen for both OHT and FHT specimens.

This phenomenon may be due to the 45º plies present in quasi-isotropic laminate. As seen in Figure 4-12, the peak longitudinal strains (e_{xx}) for CP12 are concentrated at the notch boundary and stay elevated along the longitudinal direction (due to the 0º plies). The axis of symmetry for the strains coincides with the y-axis. However, the peak strains for QI12 follow an axis approximately at a 45º angle from the y-axis. The fact that the cross-ply peak strains are pulling perpendicular to the notch boundary and those of quasi-isotropic are pulling at an angle from the notch boundary may explain why the LHE of cross-ply is higher than quasi-isotropic. Perpendicular deformation of the notch has increased leverage over the longitudinal deformation compared to deforming the notch at an angle. The peak transversal strains (e_{yy}) for CP12 are concentrated at the notch boundary and stay somewhat elevated along the longitudinal direction. This trend is similar to that exhibited in the longitudinal strain plots, however there is a clear difference. The compressive transversal strains only occur in half the specimen (the upper right side and lower left side of the notch) with no clear axis of symmetry. The quasi-isotropic layup exhibits the same 45º axis, along which the peak compressive strains are distributed. This favors an increase in THC values for quasi-isotropic compared to cross-ply layups. CP12 and QI12 were used as an example, CP8 and QI8 exhibit the same phenomenon. The strain contour plots for CP8 and QI8 can be seen in Appendix A.

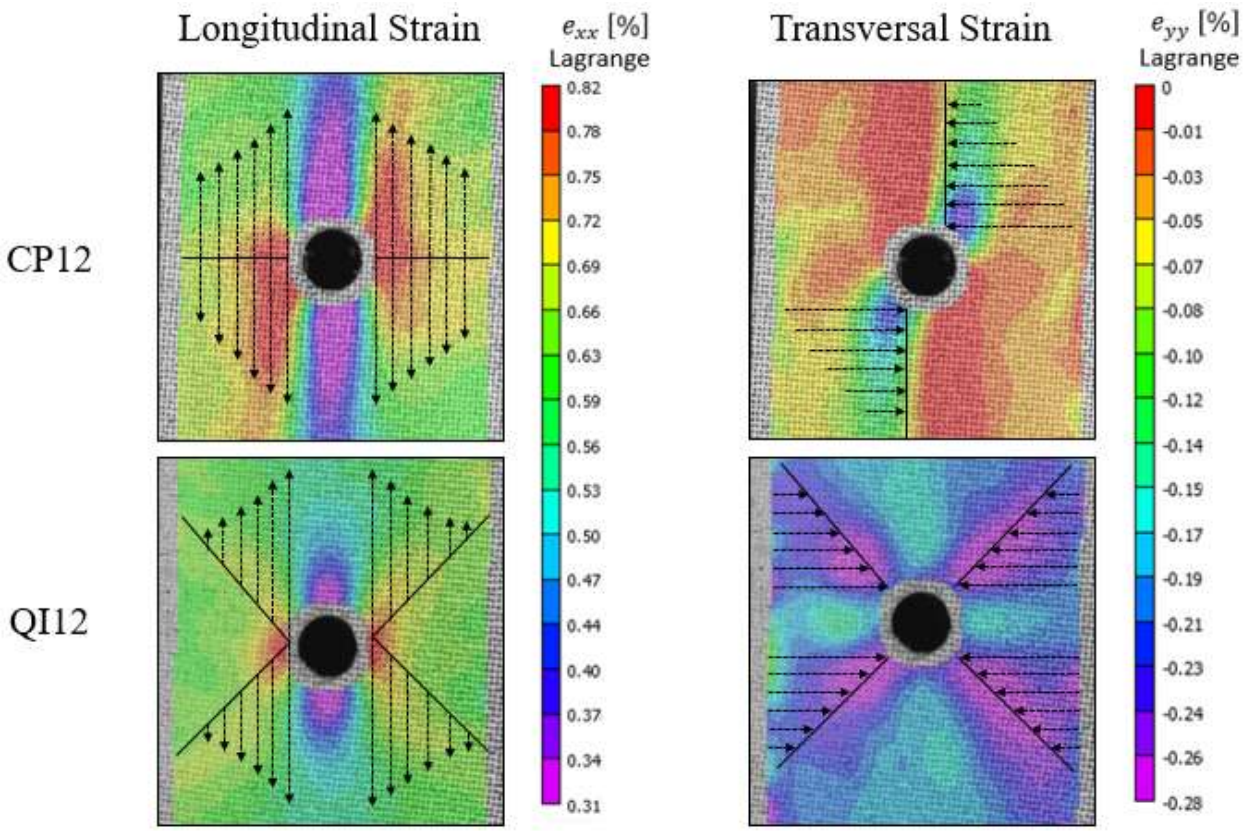

Figure 4-12: Longitudinal and transversal strain contours at 40% OHT/TS for CP12 and QI12

CHAPTER 5 CONCLUSION AND RECOMMENDATIONS

5.1 Conclusion

An experimental and analytical investigation into the stress distribution, stress concentration factors (SCFs) and hole deformation of open- and filled-hole carbon/epoxy cross-ply and quasi-isotropic laminates with varying thicknesses was carried out using digital image correlation (DIC) strain measurements. Experimental SCFs and tensile strengths were compared to analytical results calculated using the average and point stress criteria. Notch deformation was measured using virtual extensometers in the longitudinal and transversal directions across the notch of composite laminates. The sub-objectives of this research are to characterize the strength, SCFs, stress distribution and notch deformation. The important findings of this study are described in the following sections.

Open- and Filled-Hole Tensile Strength Characterization

- Increasing the thickness of a laminate will reduce its tensile strength in OHT specimens. This agrees well with [1,2]. Using sub laminate thickening (which is used in this research) disperses the 0º plies uniformly through the thickness of the laminate and aids in halting the propagation of sub-critical damage. Therefore, as the laminate thickness increases, the sub-critical damage decreases. This causes a lack of stress relief away from the notch and thus the tensile strength decreases.
- FHT specimens all have lower tensile strength than their OHT counterparts, except for CP12. Considering the fact that thicker CP laminates are less prone to damage than thinner CP laminates, introducing a clamped bolt may not affect the strength in an adverse way. The variance in tensile strength is slight, and it can therefore be concluded that filling a notch with a clamped bolt does not greatly reduce or increase the tensile strength. This agrees with the findings in [5].
- Filling the notch with a clamped bolt generates a stiffening effect for the CP8 and QI12 laminate. OHT CP8 is less stiff than FHT CP8 and the same is seen in QI12. This may be due to the bolt delaying the deformation of the notch, which will create an increased stiffening effect.

Stress Distribution Characterization

- Using digital image correlation (DIC) strain measurements for plotting stress distribution in notched composite plates is quite effective. The results compare well to Lekhnitskii's analytical model [7].
- Thinner OHT cross-ply laminates (CP8) have better stress distribution capabilities than their thicker counterparts (CP12), whereas thicker quasi-isotropic laminates (QI12) are better at distributing stress than thinner ones (QI8).
- Filling the notch with a clamped bolt (FHT specimens) brings the stress distribution capabilities of cross-ply and quasi-isotropic layups to align with one another. The clamping load of the bolt nullifies any effects that the lay-up or thickness has on the stress distribution capability when compared to OHT specimens.

Stress Concentration Factors Characterization

- As expected, cross-ply layups have higher stress concentration factors (SCFs) than quasi-isotropic layups due to the increased number of 0^{o} plies, which are in the direction of the applied load.
- Thinner OHT laminates have smaller SCF values than their counterparts, since thinner laminates exhibit more damage due to the decreased number of 0^{o} plies.
- Thinner FHT specimens (CP8 and QI8), have approximately a 5% increase in their SCFs when compared to OHT specimens. This is due to the clamping load that supports the integrity of the notch and does not allow the same stress relief at the notch boundary as seen in OHT specimens. The SCFs of thicker laminates (CP12 and QI12) are not as affected by the inclusion of a tightened bolt. We observed that the SCF of CP12 FHT is lower than that of its OHT and the difference in variation of the SCFs of QI12 between OHT and FHT is negligible. This may be because thinner laminates are more adversely affected by damage then their thicker counterparts.

- The point stress criterion (PSC) gives a very good approximation of the stress concentration factors for all laminates investigated.
- The average stress criterion (ASC) has induced errors greater than 13% for OHT and 15% for FHT when estimating cross-ply laminates. For quasi-isotropic laminates however, the ASC estimates are as accurate as those obtained using the PSC.
- The PSC overestimates, whereas the ASC underestimates the stress concentration factor when compared to the experimental results. The PSC can therefore be used for a more conservative analysis.

Notch Deformation Characterization

- Throughout the range of applied tensile load, the longitudinal hole elongation (LHE) of cross-ply layups was greater than that of quasi-isotropic layups (approximately 100% more). This is quite interesting as the opposite was expected since cross-ply laminates have higher rigidity than quasi-isotropic laminates. This phenomenon was exhibited in both OHT and FHT specimens.
- The transversal hole compression (THC) of cross-ply layups was less than quasi-isotropic layups (approximately 75% less). This is counter-intuitive to the findings mentioned previously for the LHE of cross-ply and quasi-isotropic laminates; a notch that has greater LHE was expected to have higher THC. To the author's knowledge this phenomenon has not been identified in the literature.
- These phenomena may be explained by the fact that the inclusion of the 45º plies in the quasi-isotropic layup induces a butterfly distribution of peak strain around the notch area, which contributes more to the transversal compression of the notch than its longitudinal elongation.

5.2 Limitations

A limitation to this research is the fact that the digital image correlation technique lacks the ability to retrieve strain values directly at the notch boundary. That being said, the DIC is one of the few techniques that can retrieve full-field strain values near and around the boundary of the notch. Strain gauges and extensometers do not provide this capability.

It was assumed that unidirectional plies were used when calculating the material properties, when in fact woven plies were investigated. This may induce some errors within the material characteristic calculations and these errors will trickle down into the calculations of the stress distribution. As well, Test Method II described in ASTM D3171 was used to calculate the volume fiber fraction (V_f) of the laminates. This test method assumes that no porosity (air bubbles) is present within the laminate. It does not consider the volume fraction of porosity.

5.3 Recommendations

It is recommended to create a finite element model for the open- and filled-hole specimens to be able to obtain a quantitative explanation of the difference in notch deformation of the cross-ply and quasi-isotropic layups investigated in this thesis.

It would be interesting to analyze the stress distribution and notch deformation of single-lap single-bolted joints and to compare the results to those stated in this work. The stress distribution calculation for single-lap joints would not come without its own difficulties, since secondary bending and the associated stresses must be considered and quantified to be able to accurately calculate the stress at the surface of the joint. Using the digital image correlation technique may enable capturing out-of-plane deformation, however a finite element model would be critical to verify the experimental results.

BIBLIOGRAPHY

[1] Green B. G., Wisnom M. R., Hallett S. R., "An experimental investigation into the tensile strength scaling of notched composites," Composites Part A, 38, 2007, pp. 613-624.

[2] O'Higgins R. M., McCarthy M. A., McCarthy C. T., "Comparison of open hole tension characteristics of high strength glass and carbon fibre-reinforced composite materials," Composite Science and Technology, 68 2008, pp. 2770-2778.

[3] Hallet S. R., Wisnom M. R., "Experimental investigation of progressive damage and the effect of layup in notched tensile tests," Journal of Composite Materials, 40(2), 2006, pp. 119-141.

[4] Hao A., Yuan L., Chen J. Y., "Notch effects and crack propagation analysis on kenaf/polypropylene nonwoven composites," Composites Part A, 73, 2015, pp. 11-19.

[5] Gamdani F., Boukhili R., Vadean A., "Tensile strength of open-hole, pin-loaded and multi-bolted single-lap joints in woven composite plates," Materials and Design, 88, 2015, pp. 702-712.

[6] Yan Y., Wen W.-D., Chang F.-K., Shyprykevich P., "Experimental study on clamping effects on the tensile strength of composite plates with a bolt-filled hole," Composites Part A, 30, 1999, pp.1215-1229

[7] Lekhnitskii G., Tsai W. S., Cheron T., "Anisotropic plates," New York; Gordon and Breach Science Publishers, 1968.

[8] Whitney J. M., Nuismer R. J., "Stress fracture criteria for laminated composites containing stress concentrations," Journal of Composite Materials, 8, 1974, pp. 253-265.

[9] Nuismer R. J., Whitney J. M., "Uniaxial failure of composite laminates containing stress concentrations," Fracture Mechanics of Composites, ASTM, 1975, pp. 117-142.

[10] Pipes R. B., Wetherhold R. C., Gillespie J. W., "Notched strength of composite materials," Journal of Composite Materials, 13, 1979, pp. 148−160.

[11] Kim J.K., Kim D. S., Takeda N., "Notched strength ad fracture criterion in fabric composite plates containing a circular hole," SAGE for American Society for Composites, 1995, pp. 982-998.

[12] Awerbuch J., Madhukar M. S., “Notched strength of composite laminates: Predictions and Experiments – A Review,”, Journal of Reinforced Plastics and Composites, 4, 1995, pp. 3-158.

[13] Waddoups M. E, Eisenmann J. R., Kaninski B. E., “Microscopic fracture mechanisms of advanced composite materials,” Journal of Composite Materials, 5, 1971, pp. 446−454.

[14] Mar J. W., Lin K. Y., “Fracture mechanics correlation for tensile failure of filamentary composites with holes,” Journal of Aircraft, 14, 1977, pp. 703−704.

[15] Chang F. K., Chang K. Y., “A Progressive damage model for laminated composites containing stress concentrations,” Journal of Composite Materials, 21, 1987, pp. 834−855.

[16] Tan S. C., “A progressive failure model for composite laminates containing openings,” Journal of Composite Materials, 25, 1991, pp. 536−577.

[17] Srivastava V. K., “Notched strength prediction of laminated composite under tensile loading,” Journal of Materials Science and Engineering, A328, 2002, pp. 302-309.

[18] Ko W. L., “Stress concentration around a small circular hole in the HiMAT composite plate,” NASA 1985.

[19] Dirikolu M. H., Aktas A., “Analytical and finite element comparisons of stress intensity factors of composite materials”, Composite Structures, 50, 2000, pp. 99-102

[20] Tan S. C., “Finite-width correction factors for anisotropic plate containing a central opening,” Journal of Composite Materials, 22, 1988, pp. 1080-1097.

[21] Toubal L., Karama M., Lorrain B., “Stress concentration in a circular hole in composite plate,” Composite Structure, 68, 2005, pp. 31-36.

[22] Khechai A., Tati A., Guerira B., Guettala A., Mohite P.M., “Strength degradation and stress analysis of composite plates with circular, square and rectangular notches using digital image correlation”, Composite Structures, 185, 2018, pp. 699-715.

[23] Duan S., Zhang Z., Wei K., Wang F., Han X., “Theoretical study and physical test of circular hole-edge stress concentration in long glass fiber reinforced polypropylene composite”, Composite Structures, 236, 2020, 111884.

[24] Gao X., Yu G., Xue J., Song Y., “Failure analysis of C/SiC composites plate with a hole by the PFA and DIC method”, Ceramics International, 43, 2017, 5255-5266.

[25] Ray-Chaudhuri S., Chawla K., “Stress and strain concentration factors in orthotropic composites with hole under uniaxial tension,” Curved and Layered Structures, 5, 2018, pp. 213-231.

[26] Whitney J. M., Kim R. Y., “Composite materials: testing and design,” (Fourth Conference), ASTM STP, 229, 1977, pp. 617

APPENDIX A: ADDITIONAL STRAIN CONTOUR PLOTS

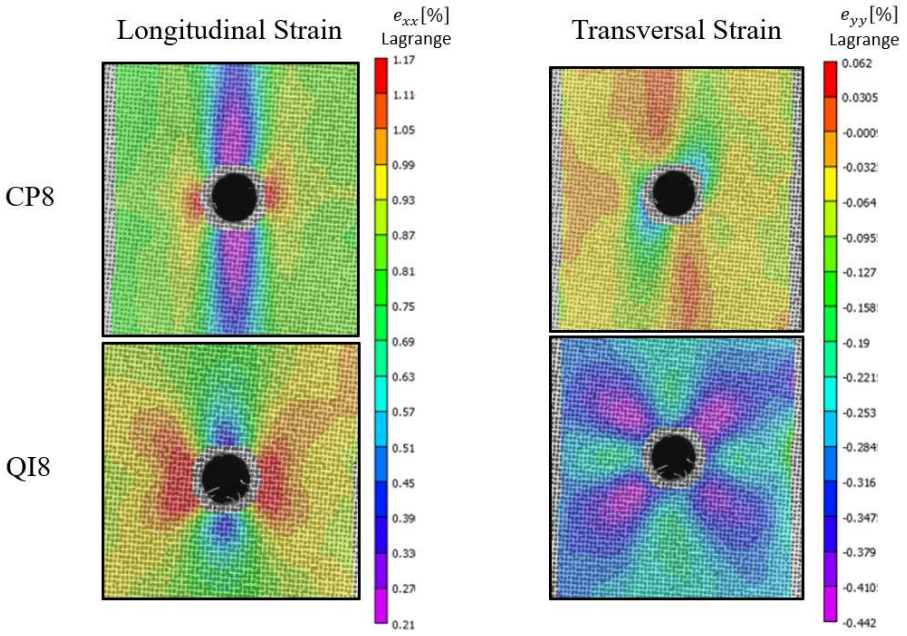

Figure A- 1 : Longitudinal and transversal strain contours at 40% OHT/TS for CP8 and QI8

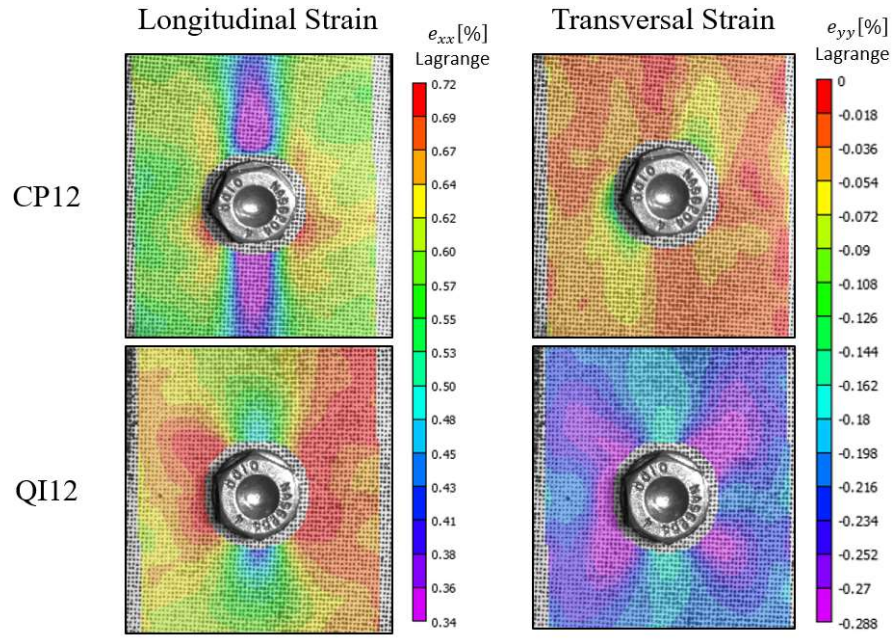

Figure A- 2: Longitudinal and transversal strain contours at 40% FHT/TS for CP12 and QI12

APPENDIX B: MATERIAL PROPERTIES

The following discusses, in detail, the methodology and calculations of the material properties for the composite specimens tested and analyzed in this thesis, which are 8- and 12-layer cross-ply (CP8 and CP12) and quasi-isotropic (QI8 and QI12) carbon fiber woven laminates.

Fiber and Matrix Properties

The fiber tensile modulus (E_f) and Poisson ratio (υ_f) as well as the matrix tensile modulus (E_m) and the matrix Poisson ratio (υ_m) are retrieved from data sheets and the values are tabulated in Table B.1.

Table B.1: Carbon-fiber and epoxy material properties

Fiber and Matrix Properties	Values	Material Name
E_f	230 GPa	T300 carbon fiber
υ_f	0,2	
E_m	2,10 GPa	Araldite epoxy resin
υ_m	0,35	

The fiber volume fraction (V_f) and the matrix volume fraction (V_m) are estimated using Test Method II described in ASTM D3171. The calculations were done for CP8, CP12, QI8 and QI12 as seen in Table B.2.

Table B.2: Fiber and matrix volume fraction

Laminate	V_f [%]	V_m [%]
CP8	50,21	49,79
CP12	51,47	48,53
QI8	50,65	49,35
QI12	50,51	49,49

Lamina Properties

From the values in Table B.1 and Table B.2, the tensile modulus and the Poisson ratio in the longitudinal (E_{11} , υ_{12}) and transversal (E_{22}, υ_{21}) direction of the lamina from each configuration are shown in Table B.3 and are calculated as follows:

$$E_{11} = E_f V_f + E_m V_m \tag{B1}$$

$$\upsilon_{12} = \upsilon_f V_f + \upsilon_m V_m \tag{B2}$$

$$E_{22} = \frac{E_f E_m}{E_f V_m + E_m V_f} \tag{B3}$$

$$\upsilon_{21} = \frac{E_{22}}{E_{11}} \upsilon_{12} \tag{B4}$$

Table B.3: Longitudinal and transversal Young's modulus and Poisson ratio for a lamina

Lamina	E_{11}[GPa]	E_{22}[GPa]	υ_{12}	υ_{21}
Carbon/Epoxy	117,66	4,22	0,275	0,01

The fiber shear modulus (G_f) and the matrix shear modulus (G_m) are estimated using their respective Young's modulus and Poisson ratio with the following equation:

$$G = \frac{E}{2(1+\nu)} \tag{B5}$$

The lamina in-plane shear modulus (G_{12}) is calculated assuming an isotropic relation:

$$G_{12} = \frac{G_f G_m}{G_f V_m + G_m V_f} \tag{B6}$$

The values of G_f, G_m and G_{12} are shown in Table B.4.

Table B.4: Shear Modulus

Lamina	G_f [GPa]	G_m [GPa]	G_{12} [GPa]
Carbon/Epoxy	95,83	0,78	1,55

The stiffness matrix $[Q]$ for a specially orthotropic lamina is represented as:

$$[Q] = \begin{bmatrix} Q_{11} & Q12 & 0 \\ Q_{21} = Q_{12} & Q22 & 0 \\ 0 & 0 & Q_{66} \end{bmatrix} \tag{B7}$$

Where,

$$Q_{11} = \frac{E_{11}}{1 - \upsilon_{12}\upsilon_{21}} \tag{B8}$$

$$Q_{22} = \frac{E_{22}}{1 - \upsilon_{12}\upsilon_{21}} \tag{B9}$$

$$Q_{12} = Q_{21} = \frac{\upsilon_{12}E_{11}}{1 - \upsilon_{12}\upsilon_{21}} = \frac{\upsilon_{21}E_{22}}{1 - \upsilon_{12}\upsilon_{21}} \tag{B10}$$

$$Q_{66} = G_{12} \tag{B11}$$

When incorporating angled plies, the stiffness matrix for a general orthotropic lamina $[\bar{Q}]$ is:

$$[\bar{Q}] = \begin{bmatrix} \bar{Q}_{11} & \bar{Q}_{12} & \bar{Q}_{16} \\ \bar{Q}_{12} & \bar{Q}_{22} & \bar{Q}_{26} \\ \bar{Q}_{16} & \bar{Q}_{26} & \bar{Q}_{66} \end{bmatrix} \tag{B12}$$

The constituents of the above-mentioned matrix can be denoted by:

$$\bar{Q}_{11} = U_1 + U_2 \cos 2\theta + U_3 \cos 4\theta \tag{B13}$$

$$\bar{Q}_{12} = U_4 - U_3 \cos 4\theta \tag{B14}$$

$$\bar{Q}_{22} = U_1 - U_2 \cos 2\theta + U_3 \cos 4\theta \tag{B15}$$

$$\bar{Q}_{16} = \frac{1}{2} U_2 \sin 2\theta + U_3 \sin 4\theta \tag{B16}$$

$$\bar{Q}_{26} = \frac{1}{2} U_2 \sin 2\theta - U_3 \sin 4\theta \tag{B17}$$

$$\bar{Q}_{66} = U_5 - U_3 \cos 4\theta \tag{B18}$$

Where U_1, U_2, U_3, U_4 and U_5 are angle-invariant stiffness properties and are calculated with the elements from the stiffness matrix $[Q]$ for a specially orthotropic lamina, as shown below:

$$U_1 = \frac{1}{8}(3Q_{11} + 3Q_{22} + 2Q_{12} + 4Q_{66}) \tag{B19}$$

$$U_2 = \frac{1}{2}(Q_{11} - Q_{22}) \tag{B20}$$

$$U_3 = \frac{1}{8}(Q_{11} + Q_{22} - 2Q_{12} - 4Q_{66}) \tag{B21}$$

$$U_4 = \frac{1}{8}(Q_{11} + Q_{22} + 6Q_{12} - 4Q_{66}) \tag{B22}$$

$$U_5 = \frac{1}{2}(U_1 - U_4) \tag{B23}$$

Laminate Properties

The theory mentioned previously was used for the estimation of lamina properties. To calculate the mechanical properties of a laminate (the stacking of multiple lamina), the extension stiffness matrix [A], the coupling stiffness matrix [B] and the bending stiffness matrix [D] must be calculated.

The extension stiffness matrix [A] is calculated from:

$$A_{mn} = \sum_{j=1}^{N} (\bar{Q}_{mn})_j (h_j - h_{j-1}) \tag{B24}$$

The coupling stiffness matrix [B] is calculated from:

$$B_{mn} = \frac{1}{2}\sum_{j=1}^{N} (\bar{Q}_{mn})_j (h_j^2 - h_{j-1}^2) \tag{B25}$$

The bending stiffness matrix [D] is calculated from:

$$D_{mn} = \frac{1}{3}\sum_{j=1}^{N} (\bar{Q}_{mn})_j (h_j^3 - h_{j-1}^3) \tag{B26}$$

Where,

- N is the total number of laminas in the laminate
- $(\bar{Q}_{mn})_j$ is the element in the $[\bar{Q}]$ matrix of the j^{th} lamina
- h_j is the distance from the midplane of the laminate to the top of the j^{th} lamina
- h_{j-1} is the distance from the midplane of the laminate to the bottom of the j^{th} lamina

It is important to note that woven plies are used as opposed to unidirectional plies. A woven lamina is similar to having two unidirectional plies perpendicular and stacked upon one another. Therefore, the number of plies, N, must be multiplied by twice the number of woven plies used if it is to be applied to a laminate with woven laminas. This estimation is considered non-conservative as the material properties calculated with this method do not account for the stress induced in the matrix by the straightening of the fibers when the laminate undergoes loading in the fiber direction. An example of this method applied to a cross-ply 8-layer (CP8) woven laminate can be seen in Figure B-1.

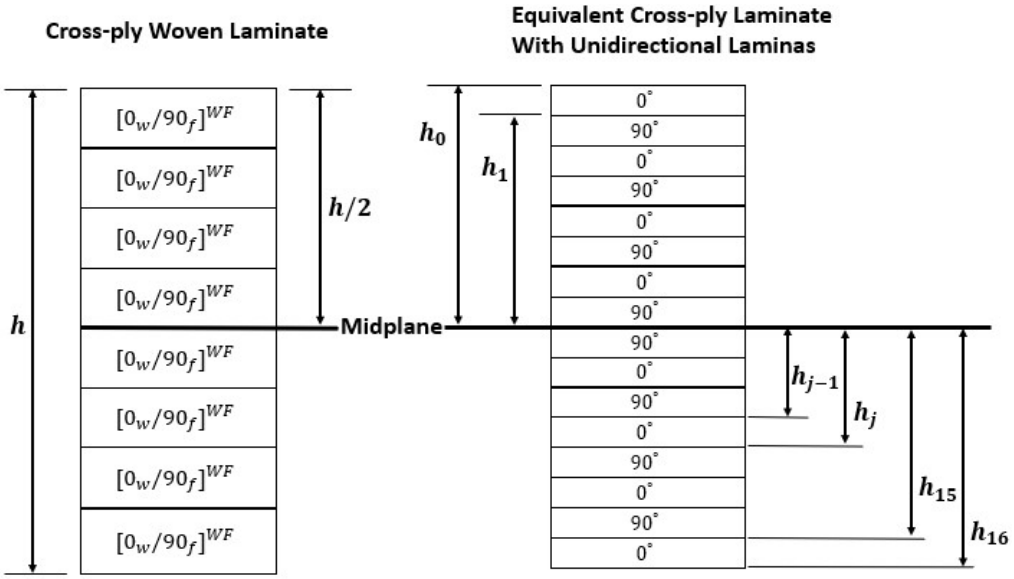

Figure B-1: Equivalent Laminate Theory